Manuscript Details

Manuscript number	BIOELECHEM_2020_105_R1
Title	Covalent immobilization of delipidated human serum albumin on poly(pyrrole-2-carboxylic) acid film for the impedimetric detection of perfluorooctanoic acid
Article type	Research Paper

Abstract

The immobilization of biomolecules at screen printed electrodes for biosensing applications is still an open challenge. To enrich the toolbox of bioelectrochemists, graphite screen printed electrodes (G-SPE) were modified with an electropolymerized film of pyrrole-2-carboxilic acid (Py-2-COOH), a pyrrole derivative rich in carboxylic acid functional groups. These functionalities are suitable for the covalent immobilization of biomolecular recognition layers. The electropolymerization was first optimized to obtain stable and conductive polymeric films, comparing two different electrolytes: sodium dodecyl sulphate (SDS) and sodium perchlorate. The G-SPE modified with Py-2-COOH in 0.1 M SDS solution showed the required properties and were further tested. A proof-of-concept study for the development of an impedimetric sensor for perfluorooctanoic acid (PFOA) was carried out using the delipidated human serum albumin (hSA) as bioreceptor. The data interpretation was supported by size exclusion chromatography and small-angle X-ray scattering (SEC-SAXS) analysis of the bioreceptor-target complex and the preliminary results suggest the possibility to further develop this biosensing strategy for toxicological and analytical studies.

Keywords	pyrrole-2-carboxylic acid; impedimetric sensor; biosensor; electropolymerization; perfluorooctanoic acid; human serum albumin.
Manuscript category	Electrified Interfaces and Biosensing
Corresponding Author	Giulia Moro
Order of Authors	Giulia Moro, Fabio Bottari, Stefano Liberi, Sonia Covaceuszach, Alberto Cassetta, Alessandro Angelini, Karolien De Wael, Ligia Maria Moretto
Suggested reviewers	Mirella Di Lorenzo, Ievgen Mazurenko, Rebeca Miranda

Submission Files Included in this PDF

File Name [File Type]

Cover_Letter_GM.pdf [Cover Letter]

Comments-BioEC-AR0329.docx [Response to Reviewers]

Highlights-Py-2-COOH.docx [Highlights]

GA-Py.tif [Graphical Abstract]

Manuscript-BioEC-AR0329.docx [Manuscript File]

Fig.1bis.tiff [Figure]

Fig.2.tiff [Figure]

Fig3.tif [Figure]

Fig.4.tiff [Figure]

Conflict of interest statement.docx [Conflict of Interest]

SM-BioEC-AR0329.docx [Supporting File]

To view all the submission files, including those not included in the PDF, click on the manuscript title on your EVISE Homepage, then click 'Download zip file'.

Università
Ca'Foscari
Venezia

**Dipartimento
di Scienze Molecolari
e Nanosistemi**

Via Torino 155
30172 Mestre (Venezia)

T +39 0412348535/8698
F +39 0412348517/8594

dsmn@unive.it

www.unive.it/dsmn

Cod. Fisc. 80007720271
P.IVA/VAT 00816350276

Venice, 21/02/2019

Dear Editors,

We would like to submit our paper titled:

Covalent immobilization of delipidated human serum albumin on poly(pyrrole-2-carboxilic) acid film for the impedimetric detection of perfluorooctanoic acid

by Giulia Moro, Fabio Bottari, Stefano Liberi, Sonia Covaceuszach, Alberto Cassetta, Alessandro Angelini, Karolien De Wael, Ligia Maria Moretto

for publication in the Special Issue "**Selected papers from the 9th International Workshop on Surface Modification for Chemical and Biochemical Sensing, SMCBS 2019, Zelechów, Poland, 8-12 November 2019**" of Bioelectrochemistry.

The manuscript describes the fabrication of a polymeric platform on graphite screen-printed electrodes (G-SPE) for the covalent immobilization of biomolecules via EDC/NHS chemistry. G-SPE were modified with an electropolymerized film of pyrrole-2-carboxilic acid, a pyrrole derivative rich in carboxylic acid functional groups, suitable for the covalent immobilization of biomolecular recognition layers. The electropolymerization was first optimized to obtain stable and conductive polymeric films, comparing two different electrolytes: sodium dodecyl sulphate (SDS) and sodium perchlorate. Then, a proof-of-concept study for the development of an impedimetric sensor for perfluorooctanoic acid (PFOA) was carried out using the delipidated human serum albumin (hSA) as bioreceptor. The data interpretation was supported by the SEC-SAXS analysis of the bioreceptor-target complex and the preliminary results suggest the possibility to further develop this biosensing strategy for toxicological and analytical studies.

We hereby declare that neither the manuscript nor any parts of its content are currently under consideration or published in another journal.

Università
Ca'Foscari
Venezia

**Dipartimento
di Scienze Molecolari
e Nanosistemi**

Via Torino 155
30172 Mestre (Venezia)

T +39 0412348535/8698
F +39 0412348517/8594

dsmn@unive.it

www.unive.it/dsmn

Cod. Fisc. 80007720271
P.IVA/VAT 00816350276

If you deem the manuscript appropriate for the special issue in question, we suggest the following researchers to handle the review:

1. Mirella di Lorenzo
Centre for Biosensors, Bioelectronics and Biodevices and Department of Chemical Engineering, University of Bath, Bath, BA2 7AY, United Kingdom
m.di.lorenzo@bath.ac.uk

2. Ievgen Mazurenko
Aix Marseille Univ, CNRS, BIP, UMR 7281, 31 chemin Joseph Aiguier, 13402 Marseille, France
imazurenko@imm.cnrs.fr

3. Rebeca Miranda Castro
Dpto. Química Física y Analítica, Universidad de Oviedo, Oviedo, Spain
mirandarebeca@uniovi.es

Best regards,

Giulia Moro

Dear Editors,

We would like to thank you and the reviewers for handling our manuscript. We are very pleased with the comments and suggestions received. We revised the manuscript addressing all the comments and the suggestions of the reviewers.

Below the point-to-point answers to each comment:

-**Reviewer 1**

Authors propose here the use of a G-SPE modified with poly(pyrrole-2-carboxilic) acid film as scaffolds to covalently immobilized delipidated hSA via EDC/NHS coupling to develop an impedimetric biosensor for sensitive (in nanomolar range) determination of PFOA in water samples. Authors perform careful optimization studies of the electropolymerization which led to the formation of attractive polymeric films that while providing the carboxylic acid functional groups needed for the covalent immobilization of biomolecules improve the conductivity of the working electrode. The impedimetric results (obtained by extracting the absolute impedance values at 10 Hz from the Bode phase plot) were supported the study of the hSA-PFOA complex performed by SEC-SAXS analysis.
The results obtained, interesting, novel and of great practical applicability for the development of other types of electrochemical biosensors apart from the enzymatic ones (affinity biosensors), are well discussed. Therefore, I find this paper suitable for publication in this journal, after addressing all the following major concerns:

We thank the reviewer for the clear summary and the feedback provided.

1. Please discuss the reproducibility between determinations carried out with different biosensors prepared in the same way.

Reproducibility together with selectivity and sensibility are key-issues in biosensing, however we did not discuss them in detail in the manuscript as we preferred focusing on the concept rather than optimizing the analytics of the detection. Nevertheless, it is possible to evaluate the sensor reproducibility from the data plotted in Fig. 4B (see below). Indeed, these data were obtained from triplicates using different biosensors modified with the same protocol, as suggested by the error bars reported. From this dataset it is possible to calculate an average error of c.a. 10%. To address this point, we included this value in the text, please see par. 3.2.2 sentence in red.
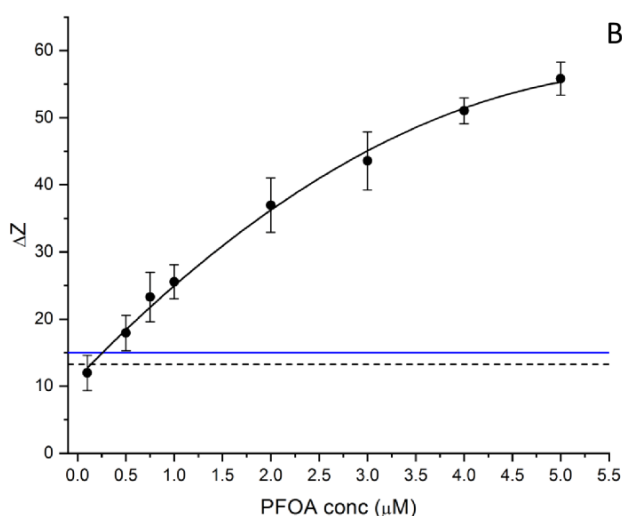
2. Please estimate LOD offered by the proposed biosensor.

As observed in Fig. 4B, the calibration plot presents a nonlinear trend and it was fitted with the polynomial equation reported in the caption ($y = 11.20 + 14.97x^1 - 1.23x^2$) and it present a linear interval between 500 nM and 2 µM. From this dataset it was not possible to calculate a meaningful LOD value, because we had only 4 points in the linear interval, which are not enough. Moreover, we found that the blank and interfering compounds signals would also affect this theoretical value. We faced this problem also in other works, where we addressed it by introducing the concept of "experimental LOD" that is the lower concentration of analyte detectable. In this case (being a proof-of-concept study with a focus on the polymeric modification), we did not use this term, but we simply showed that the lower concentration of PFOA detectable was 500 nM. Once again, we hope to improve these values in the future optimization study.

3. What is the storage stability of the hSA poly(Py-2-COOH) modified G-SPE biosensors?

The storage stability has not been tested yet. We observed a good stability in the timeframe in which the biosensors were prepared and tested, c.a. 24h. Considering that the bioreceptor stability was largely characterized even with mass spectrometry and complementary techniques, we expect to have a storage stability of one week at least.

Authors must demonstrate the selectivity of this biosensor against other PFOA analogues.

The selectivity was considered by testing a relatively high concentration of PFOS (1 µM). The perfluorooctanoic acid is together with PFOA the most studied fluorinated compound of this class of contaminants. PFOA and PFOS present a structural similarity because they are both C8 with a linear chain and they differ only for their head group (sulfonic acid for PFOS and carboxylic acid for PFOA). For this reason, we consider the PFOS as the best interfering compound to be tested aiming to address the sensor selectivity. Other fluorinated contaminants with shorter or branched chains, such as perfluorodecanoic acid (PFDA) or perfluorohexanoic acid (PFHxA), will be considered in future studies.

4. The main advantages of this biosensor over the other electrochemicals previously described for the determination of PFOA cited in the introduction [references 16-17] should be clearly stated.

All the already reported biosensors for PFOA are based on MIP and requires some other co-reactant or label to carry out the detection, as for example $S_2O_8^{2-}$ oxidizing agent for electrochemiluminescence (ref. 17). Our sensor is a protein based electrochemical biosensor which has two main advantages: it is based on a label-free detection strategy and the sensor fabrication is easy to perform and does not require complex instrumentations or time-consuming modifications protocols. A short paragraph has been added in red at the end of the introduction to stress these advantages.

5. With a view to their future practical applicability for the development of other types of biosensors with application in fields such as the clinical and the food ones, it would be interesting to evaluate the behaviour of these biosensors in biofluids or matrices with high concentrations of albumin such as serum.

We agree with the reviewer, but we need to distinguish between the hSA-based biosensor and the polymeric platform. It would be indeed very interesting to test our polymer modified electrodes with other molecular recognition layers and different real matrices. As for the impedimetric hSA biosensor, we developed it with a clear analytical application, which is natural and industrial water monitoring. The complex nature of foods and biofluids may pose a challenge especially in term of unspecific

adsorption on the richly reactive surface of our polymer. Further tests are surely needed to verify the performance of the polymer platform as biosensor substrate. This falls however outside the scope of the manuscript.

6. Do the authors have any idea in view of the extensive studies they have conducted whether there would be any possibility of controlling the spatial arrangement of the carboxylic acid functional groups? This would be particularly interesting to improve/tailor the performance of affinity biosensors (mainly in nucleic acid sensors but also in immunosensors).

We would like to thank the reviewer for this useful suggestion. Indeed, the spatial characterization of the surface functional groups is still an open challenge. We are currently trying to perform µFTIR maps at SPE with multiple sampling points, subtracting the signal of the graphite inks, to map the entire electrode surface.

-**Reviewer 2**

This paper describes the preparation of a modified electrode involving covalent immobilization of delipidated human serum albumin on poly(pyrrole-2carboxilic) acid film for the impedimetric determination of perfluorooctanoic acid as a proof of concept. It is a good paper where authors use a relatively original recognition element, and the resulting device seems work well. In my opinion, the article is publishable in Bioelectrochemistry after minor revision.

We thank the reviewer for the interesting comments and for the positive opinion expressed, we will address all points in the following lines.

Specific questions are as follows:

1. Figure 3A. The modified electrodes do not have a regular semicircular shape. This fact this fact must be taken into account to explain the behavior of these electrodes.

As the reviewer correctly pointed out, the semicircular part of the Nyquist plots presents a depressed shape, and this was taken into account in the EEC fitting by using constant phase elements (CPE) instead of pure capacitors elements. The CPE models this "non-ideal" behavior of the double layer capacitance and it is commonly used for electrode surface modified with non-homogeneous materials (i.e. polymers, biomolecules, etc.).

2. Optimization studies regarding the hSA loading on the Py-2-COOH modified electrode should be made.

The hSA loading at Py-2-COOH-G-SPE was optimized during this study considering a limited range of concentrations, from 0.5 to 5 mg/mL (please see the graph below). The comparison was performed on the value of the hSA-Rct (the EEC in Fig. 3C was used for the fitting). We notice that with a hSA concentration lower than 2 mg/mL the associate Rct values were affected by relatively high errors suggesting a non-stable modification. With 2 mg/mL a good reproducibility was obtained, while for higher concentrations of protein, hSA-Rct did not change significantly. With 5 mg/mL, we recorded an increase in the Rct but with a much higher associated error. This is possibly due to desorption phenomena. We added this graph and discussion in SM, referring to it in the first part of paragraph 3.2 (see sentences in red).
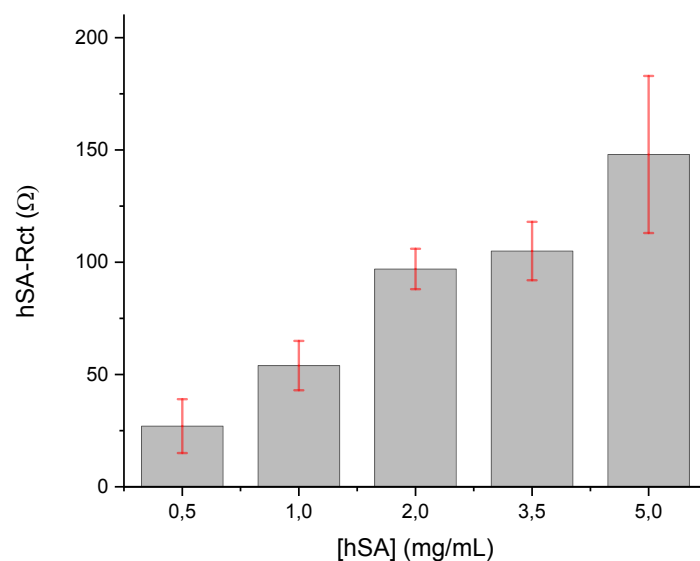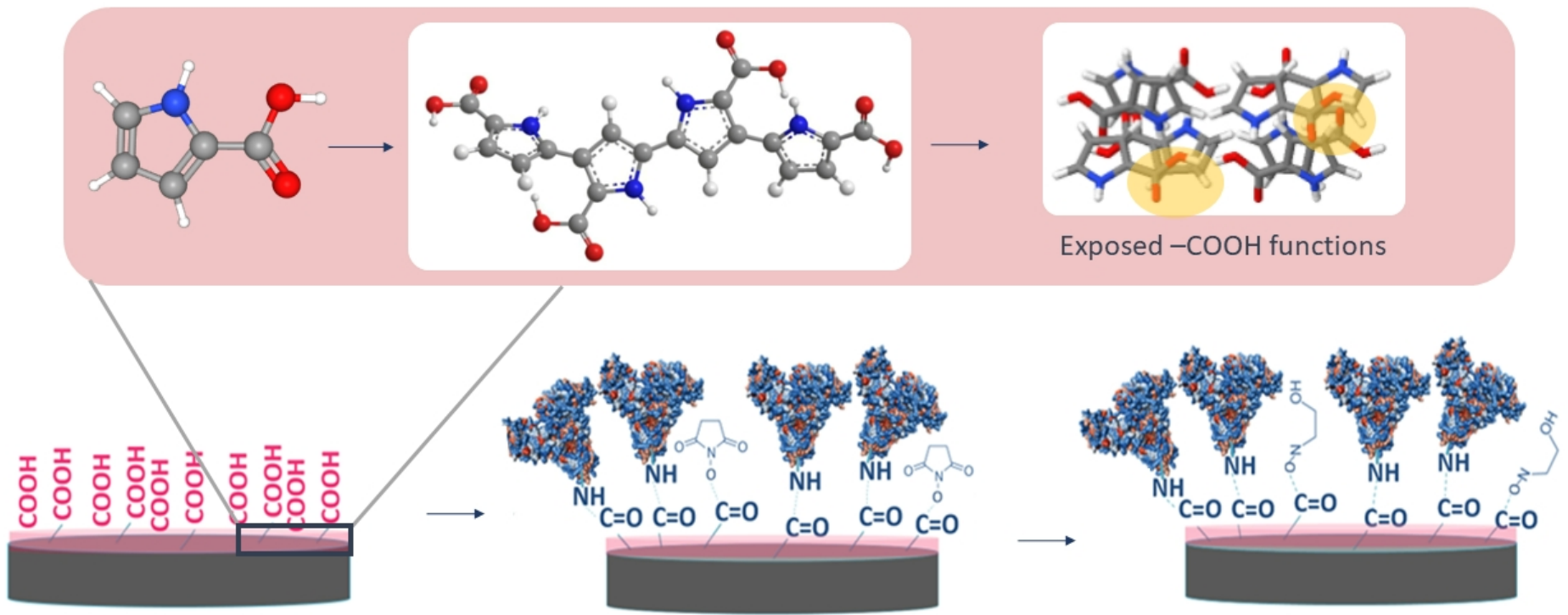
3. Although authors say it is a proof of concept, the analytical part should be completed with interference studies and a simple application to a real sample.

Both interference studies and real sample (industrial water monitoring) applicability are part of a second ongoing study. These preliminary results clearly show the need of a larger series of experiments. Concerning the possible interfering compounds, we chose to test the perfluorooctanoic acid (PFOS) because of its structural similarity with PFOA: they are both C8 with a linear chain and they differ only for their head group. For this reason, we consider the PFOS as the best interfering compound to test for a first evaluation of the sensor selectivity. This impedimetric sensors will be applied in the analysis of water samples, so we plan to remove other possible interfering compounds (salts, dispersed particles) by including a suitable sample pretreatment in the analytical protocol.

4. The number of references is excessive. Authors should only cite those papers closely related to the subject of research.

We reduced the number of references, especially in the introduction. However, we consider the rest of the bibliography very important to help the reader follow our experimental work, giving the rationale behind many of our choices (e.g. electropolymerization parameters or equivalent circuit fittings).

Highlights:

- G-SPE were modified with Py-2-COOH for the covalent immobilization of delipidated hSA.

- Impedimetric detection of perfluorooctanoic acid binding to delipidated hSA.

- Polymer modified G-SPE for biosensing applications.

Exposed −COOH functions

Covalent immobilization of delipidated human serum albumin on poly(pyrrole-2-carboxylic) acid film for the impedimetric detection of perfluorooctanoic acid

Giulia Moro [a,b,c,1*], Fabio Bottari [b,c,1], Stefano Liberi [a], Sonia Covaceuszach [d], Alberto Cassetta [d], Alessandro Angelini [a,e], Karolien De Wael [b,c], Ligia Maria Moretto [a]

[a] Department of Molecular Sciences and Nanosystems, Ca' Foscari University of Venice, Via Torino 155, 30172 Mestre, Italy; [b] AXES Research Group, Department of Bioscience Engineering, University of Antwerp, Groenenborgerlaan 171, 2020 Antwerp, Belgium; [c] NANOlab Center of Excellence, Groenenborgerlaan 171, 2020 Antwerp, Belgium; [d] Istituto di Cristallografia – CNR, Trieste Outstation, Italy SS 14 km 163.5, Basovizza, Trieste, Italy; [e] European Centre for Living Technology (ECLT), Ca' Bottacin, Dorsoduro 3911, Calle Crosera, 30123 Venice, Italy.

[1] These authors contributed equally to this work and should be considered co-first authors.

*Corresponding author: giulia.moro@unive.it

Abstract

The immobilization of biomolecules at screen printed electrodes for biosensing applications is still an open challenge. To enrich the toolbox of bioelectrochemists, graphite screen printed electrodes (G-SPE) were modified with an electropolymerized film of pyrrole-2-carboxilic acid (Py-2-COOH), a pyrrole derivative rich in carboxylic acid functional groups. These functionalities are suitable for the covalent immobilization of biomolecular recognition layers. The electropolymerization was first optimized to obtain stable and conductive polymeric films, comparing two different electrolytes: sodium dodecyl sulphate (SDS) and sodium perchlorate. The G-SPE modified with Py-2-COOH in 0.1 M SDS solution showed the required properties and were further tested. A proof-of-concept study for the development of an impedimetric sensor for perfluorooctanoic acid (PFOA) was carried out using the delipidated human serum albumin (hSA) as bioreceptor. The data interpretation was supported by size exclusion chromatography and small-angle X-ray scattering (SEC-SAXS) analysis of the bioreceptor-target complex and the preliminary results suggest the possibility to further develop this biosensing strategy for toxicological and analytical studies.

Keywords: pyrrole-2-carboxylic acid, impedimetric sensor, biosensor, electropolymerization, perfluorooctanoic acid, human serum albumin.

1. Introduction

Electrochemical sensors and biosensors are answering the increasing need of portable tools for the semi-quantitative detection of environmental contaminants (EC) by direct electrochemical fingerprinting or indirect sensing strategies [1]. In the broader context of EC, per- and polyfluoroalkyl substances (PFAS) represent a class of chemicals in continuous expansion (see emerging PFAS in [2,3]). PFAS and particularly perfluorooctanoic acid (PFOA) are still subjected to extensive toxicological studies to clarify their effects on the ecosystem and human health [4]. Nonetheless, previous studies already claimed their tendency to undergo bioaccumulation in vegetal and animal tissues [5] suggesting the need of large-scale, strict monitoring plans [6] and efficient water treatments [7]. For these reasons, there is an urgent demand of novel sensors for natural and industrial water monitoring, which needs to be rapid, user-friendly, robust and sensitive enough to reach the legislation limits of such EC. Electrochemical biosensors have been regarded as one of the most promising alternative to meet analogous demands in several other fields, such as point-of-care testing [8] and food safety [9].

Concerning the detection of PFOA, only few examples of electrochemical sensors have been reported up to now, mainly potentiometric [10], electrochemiluminescence [11] and photoelectrochemical [12] ones. These sensors are all based on biomimetic receptors such as the molecularly imprinted polymers (MIP) employed also in PFOA removal [13] and non-electrochemical sensing devices [14]. However, also bioreceptors can play an important role in PFOA sensing, as showed by the immunosensor developed by Cennamo *et al.* [15]. So far, protein-based bioreceptor have not been considered, although serum proteins-PFAS interactions were largely investigated [16]. In particular, PFOA capability to interact with albumin (thanks to PFOA fatty-acid mimic behaviour) was clearly stated in numerous toxicological studies [17,18] giving the opportunity to use these common proteins as a bioreceptors for PFOA sensing. Moreover, albumin-based electrochemical sensors have already showed good performances in the highly selective and sensitive detection of small molecules [19] as well as larger targets [20]. Albumin is non-electroactive and often combined with impedimetric affinity-based sensors, where the bioreceptor is first immobilized on the electrode surface, detecting the protein-target interaction as a localized change in the electrode-solution interface [21]. However, the immobilization of the bioreceptor is usually a bottleneck in the development of new sensors, particularly at screen printed electrode. To overcome this issue, other surface modifiers are often included to guarantee the stability of the immobilization as well as the electrode surface conductivity and consequently the device sensitivity. Zamani *et al.* [22] recently reviewed the preeminent role of conductive electropolymerized polymers, especially pyrrole and its derivatives, that were extensively studied and applied as electrode modifiers [23]. Among the pyrrole derivates, pyrrole-2-carboxylic acid (Py-2-COOH) was less employed in electroanalytical applications [24–26], even possessing many sought-after characteristics compared to the parent compound pyrrole, such as the presence of the carboxylic acid functional groups which can be used to couple amide-bearing molecules to the surface via EDC/NHS chemistry. The complete characterization of the electrochemical polymerization pathway of Py-2-COOH has been previously reported [27]. The results obtained by Foschini *et al.* [27] allowed to conclude that the electropolymerization mechanism is very similar to the one of pyrrole, as reported by Dias *et al.* [28]. The final polymeric chain will present a torsion angle between subsequent monomeric units of 74°, compared to 54° of pyrrole [27]. Thus, the electropolymerization conditions already reported and studied for pyrrole can also be applied to the polymerization of Py-2-COOH. Considering the specific electron transfer properties of polypyrrole, the conductivity of the resulting film is influenced by the electrolyte in which the electropolymerization takes place [28]. The polypyrrole film is doped with about 20-30% of anions coming from the electrolyte, and the conductivity is linked to the exchange of trapped anions between the film and the solution [29]. Moreover, acid anions increase the conductivity, while basic ones decrease it [30]. Also

the size of the anion is important for the growth of the film and its performances, such as stability to overoxidation [31]. All these parameters need to be taken into account to design suitable poly(Py-2-COOH) modification protocol compatible with graphite screen-printed electrodes (G-SPE).

Aiming to obtain stable and conductive poly(Py-2-COOH) on the electrode surface for the covalent immobilization of biomolecules, we first optimized the main electropolymerization parameters based on previously reported data [32–34]. In particular, the comparison of two different electrolytes, one organic (SDS) and another inorganic (NaClO$_4$), allowed understanding the influence of the anions on the conductivity of the obtained films at G-SPE. The optimized poly(Py-2-COOH) was then tested in an impedimetric biosensing platform. Delipidated human serum albumin (hSA) was selected as bioreceptor for PFOA sensing. The delipidation treatment, removing the fatty acids embedded in the protein, increase the available bindings site for PFOA [35], improving also the batch-to-batch reproducibility of the bioreceptor. The binding event was followed by electrochemical impedance spectroscopy (EIS) and the changes in the hSA-PFOA complex conformation were verified by SEC-SAXS (Size Exclusion Chromatography-Small-Angle X-ray Scattering). This proof-of-concept application confirmed the possibility to develop simple biosensing tools at poly(Py-2-COOH) modified G-SPE for small molecules detection, such as PFOA. This detection strategy for PFOA, based on protein bioreceptor, offers two main advantages over the already reported electrochemical biosensors: it is label-free, not requiring any label or co-reactant to perform the detection and has the potential to be an easy, fast and robust method of fabrication, based on disposable screen printed electrode and not requiring complex instrumentations or time consuming modification protocols.

2. Materials and Methods

Pyrrole-2-carboxylic acid (99%) (Py-2-COOH), perfluorooctanoic acid (PFOA, ≥96%), perfluorooctanesulfonic acid potassium salt (PFOS, ≥98%) and hydroxylamine were purchased from Sigma−Aldrich Ltd (Belgium). 1-ethyl-3-(3-dimethylamino) propyl carbodiimide hydrochloride (EDC) and N-hydroxysulfosuccinimide (NHS) were purchased from TCI (Europe). Highly purified delipidated human serum albumin (hSA) was obtained following the protocol reported in [36]. All the other reagents were of analytical grade and used as received. The 0.1 M phosphate buffer saline pH 7.4 with 0.01 NaCl was prepared by mixing stock solutions of 0.1 M NaH$_2$PO$_4$ and 0.1 M Na$_2$HPO$_4$, purchased form Sigma Aldrich. All aqueous solutions were prepared using MilliQ water (R > 18 MΩ cm). Electrochemical impedance spectroscopy (EIS) and cyclic voltammetry (CV) measurements were performed using an Autolab potentiostat/galvanostat (PGSTAT 302N, ECOCHEMIE, The Netherlands) controlled by NOVA 1.1 software. Disposable graphite screen-printed electrodes (G-SPE) consisting of a graphite working (3 mm diameter) and counter electrode and a silver pseudo reference electrode were purchased from Italsens (Florence, Italy).

2.1 G-SPE Py-2-COOH modification and characterization

The electropolymerization of 10 mM Py-2-COOH was performed by CV, using the following parameters: a potential window between -0.3 V and +1.2 V, at different scan rates (25, 50, 100 mV/s) and number of cycles (5, 10, 20).Two different electrolytes were tested namely 1 M NaClO$_4$ and 0.1 M SDS, both in aqueous solution. EIS measurements were recorded in 0.1 M phosphate buffer pH 7.4 with 2 mM [Fe(CN)$_6$]$^{3-/4-}$, in the frequency range between 0.1 MHz and 0.1 Hz, with 0.01 V amplitude and bias potential determined by open circuit potential. The EIS data were verified for linearity with the Kramers-Kronig transformation [37,38] and analysed using ZView 2. Except where otherwise stated, all the potentials are referred to silver pseudo reference electrodes (-200 mV compared to SCE). All electrochemical experiments were performed at room temperature. The modified and bare G-SPE morphology was characterized by scanning electron

microscopy (SEM). SEM images were acquired with a Field Emission Gun – Environmental Scanning Electron Microscope equipped with an Energy Dispersive X-Ray detector (FEI Quanta 250, USA).

2.2 Covalent immobilization of hSA bioreceptor

A volume of 50 µL of 10 mM Py-2-COOH in 0.1 M SDS aqueous solution was placed on the G-SPE and the electropolymerization was performed by CV (5 cycles at 100 mV/s). The modified G-SPE were first rinsed with 1 mL phosphate buffer pH 7.4. To activate the carboxylic acid groups, 20 µL of an equimolar solution (0.07 M) of EDC/NHS in MilliQ water were incubated at the working electrode for 20 min keeping the G-SPE at 4° C. The solution was removed and 30 µL of 2 mg/mL delipidated hSA in phosphate buffer pH 7.4 were let in contact with the working electrode for 30 min at 4° C. The hSA modified G-SPE were rinsed with 1 mL phosphate buffer pH 7.4 to remove the protein excess. Then, the unreacted carboxylic acid groups were blocked with 20 µL of 1 M hydroxylamine [39] incubation for 20 min at 4° C. After hSA immobilization, the G-SPE were characterized by EIS before being incubated with PFOA solutions.

2.3 Analytical protocol for PFOA detection

The modified electrode (hSA-Py-2-COOH-G-SPE) was incubated with 20 µL of PFOA solution at different concentrations for 20 min at RT. After, the electrode was rinsed with 500 µL of phosphate buffer and EIS spectra were acquired in 80 µL of 2 mM $[Fe(CN)_6]^{3-/4-}$ in 0.1 M phosphate buffer. The calibration plot was built in the concentration range between 100 nM to 5 µM: the relevant analytical parameter ΔZ is defined as the difference in absolute impedance values, acquired at 10 Hz, between the bare hSA-Py-2-COOH-G-SPE and after the incubation with PFOA. All measurements were performed in triplicates, unless otherwise indicated.

2.4 Size Exclusion Chromatography and Small-Angle X-ray Scattering (SEC-SAXS)

The SEC-SAXS experiments were performed at the P12 beamline EMBL SAXS-WAXS at PETRAIII/DESY (Hamburg, Germany) [40]. The size exclusion chromatography (SEC) column (Superdex 200 5/150 column; GE Healthcare Life Sciences) was equilibrated with SEC-SAXS running buffer A (10 mM sodium phosphate, pH 7.4, 100 mM NaCl, 5% glycerol). A 50 µL aliquot of delipidated hSA (9 mg/mL) was applied to the column. The SEC column was then equilibrated with SEC-SAXS running solution B (buffer A plus 1 mM PFOA). Before performing the SAXS experiments on the complex, the delipidated hSA was pre-incubated with 1 mM PFOA for 30 min at room temperature and a 50 µL aliquot (9 mg/mL) was applied to the column. For each run 720 images were recorded using 1 s exposure every 1.25 s at a flow rate of 0.3 mL/min. For SEC-SAXS data, frames corresponding to delipidated hSA protein peak were identified, blank subtracted and averaged using CHROMIXS [41]. Radii of gyration (Rg), molar mass estimates and distance distribution functions P(r) were computed using the ATSAS package [42], in PRIMUS [43]. Comparison of experimental SAXS data (see Table S.M. 1) and delipidated hSA crystal structure (PDB_ID: 4K2C) [44] was performed using CRYSOL [45].

3. Results and Discussion

3.1 Electropolymerization optimization

Surface modifications of screen printed electrodes may represent a challenging task and often protocols optimized for other type of electrodes (i.e. bulk macroelectrodes) are not directly compatible with SPE [46]. Modification protocols for SPE have to be straightforward and fast, while maintaining the performances of the bulk macro electrodes. In this study, the monomer electropolymerization was carried out by CV in aqueous solution avoiding organic solvents that might affect the stability of G-SPE coatings. Taking advantage on the wealth of information already present in literature only two electrolytes were tested, representing organic and inorganic anions: $NaClO_4$ [32] and SDS [33,34]. The use of these two electrolytes was linked to the good conductivity and stability of the final poly-pyrrole films obtained. Thus, they were considered the most suited candidates for the optimization of a robust poly(Py-2-COOH) film. All the parameters tested, namely number of cycles and scan rates, were evaluated in terms of final conductivity of the obtained film as well as duration of the modification protocol and applicability.

3.1.1 *SDS versus $NaClO_4$*

The electropolymerization of 10 mM Py-2-COOH at G-SPE was performed in 1 M of $NaClO_4$ [32] and in 0.1 M SDS [33,34] by running five CV cycles at 100 mV/s. The electropolymerization patterns reported in Fig. 1A and B showed a consistent behaviour for both electrolytes: the monomer oxidation occurred at about +1.1/1.2 V and the intensity of the peak current decreased with increasing the number of CV cycles. The peak currents were comparable for both $NaClO_4$ and SDS (≈ 400 µA for the first cycle) and the electrolytes differ mainly for the oxidation peak shape (more symmetrical and resolved for $NaClO_4$ solutions) and capacitive contribution (higher for SDS solution). However, the electrochemical properties of the modified electrodes investigated by CV and EIS were found to be completely different in terms of surface conductivity. In Fig. 1C, the voltammograms recorded in 2 mM $[Fe(CN_6)]^{3-/4-}$ 0.1 M KNO_3 for bare and poly(Py-2-COOH) modified G-SPE are compared. The electropolymerization in $NaClO_4$ (blue curve in Fig. 1C) passivate the electrode surface. The films obtained in SDS (red curve in Fig. 1C) showed a current increase of about 15% for both anodic and cathodic peaks and a smaller ΔEp (from 202 mV to 112 mV) compared to the bare G-SPE (black curve in Fig. 1C) both indications of enhanced electron transfer. The striking difference in conductivity of films obtained with the two modification protocols was confirmed by EIS, as showed in Fig. 1D. The electrode modified in $NaClO_4$ solution (blue dots in Fig. 1D) presented a very high charge transfer resistance (Rct) compared to the bare (black dots in Fig. 1D) as evidenced by the large semicircle in the Nyquist plot. This suggests the formation of a more insulating polymer-solution interface. On the contrary, the SDS modified electrode presents a Rct lower than the bare G-SPE, as underlined in Fig. 1E (red dots).
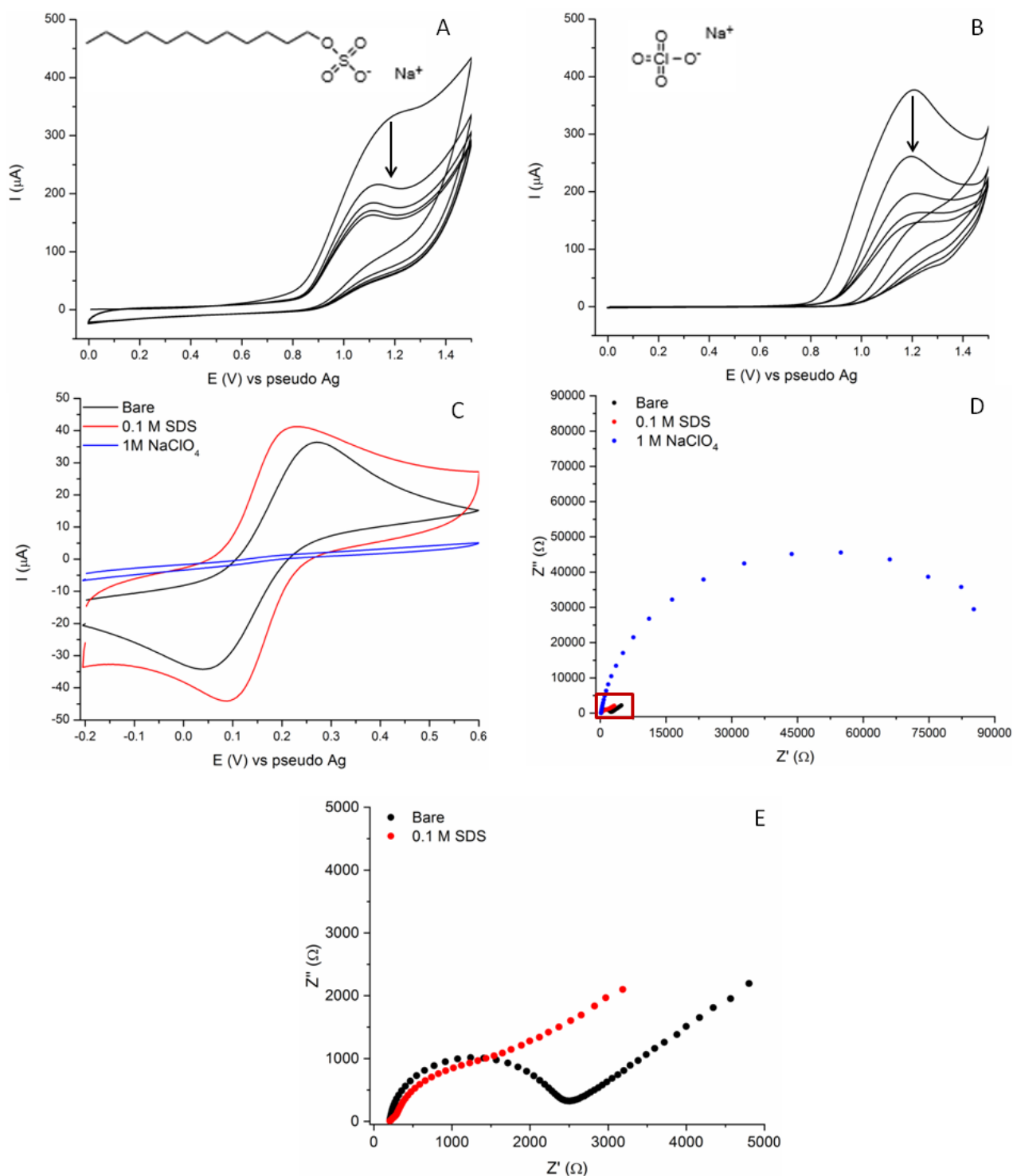
Fig. 1 Comparison of different electropolymerization patterns for 10 mM Py-2-COOH, 5 cycles at 100 mV/s between 0 and +1.5 V in 0.1 M SDS (A) and 1 M NaClO$_4$ (B); C) CVs for bare G-SPE (black line), and after 5 cycles of electropolymerization with 10 mM Py-2-COOH in 0.1 M SDS (red line) and 1 M NaClO$_4$ (blue line); D) Nyquist plot for bare G-SPE (black line), and after 5 cycles of electropolymerization with 10 mM Py-2-COOH in 0.1 M SDS (red dots) and 1 M NaClO$_4$ (blue dots); E) Magnification of Nyquist plot in Fig. 1D (region from 0 to 5000 Ω). All the measurement were performed in 0.1 M KNO$_3$ with 2 mM [Fe(CN$_6$)]$^{3-/4-}$.

Therefore, it is possible to conclude that Py-2-COOH electropolymerization in aqueous solutions is compatible with G-SPE electrodes and the polymer properties can be easily tuned using different electrolytes. In particular, the use of NaClO$_4$ leads to insulating modifiers, while with SDS the poly(Py-2-

COOH) is much more conductive. Moreover, the use of different electrolytes implies also slightly different polymer morphologies and distributions, as indicated by the SEM images reported in Fig. S.M. 1. Aiming to design a sensitive impedimetric platform, further optimization was performed only with the 0.1 M SDS electropolymerization solution.

3.1.2 Number of cycles and scan rate

The electropolymerization with SDS was optimized in terms of number of CV cycles and scan rate using a one-variable-at-a-time approach. The monomer solution, 10 mM of Py-2-COOH in 0.1 M SDS, was polymerized using increasing number of cycles (5, 10, 20) and different scan rates (25, 50, 100 mV/s). For studying the number of cycles, the scan rate was kept constant (100 mV/s) and five cycles of CV were recorded for each different scan rate value. The properties of all the modified G-SPE were characterized by CV and EIS in presence of 2 mM $[Fe(CN_6)]^{3-/4-}$, 0.1 M KNO_3.

Comparing the performances of the G-SPE modified at different number of cycles in Fig. 2A-B, it was possible to observe that the poly(Py-2-COOH) modification resulted in an higher surface conductivity compared to bare G-SPE even after 20 consecutive CV cycles. However, the best performances in terms of current intensities and ΔEp were obtained with five CV cycles (see Table S.M. 2). Increasing two or four times the number of CV cycles, there was an increment in ΔEp (from 112 mV for 5 cycles to 173 mV for the 20 cycles). To operate a rapid modification protocol, a number of five CV cycles was consider optimal for this study.

An even lower impact on the modified electrode performances was reported using different scan rates. The results presented in Fig. 2C showed a consistent behaviour with current variations of ± 11% and ΔEp differences of maximum 22 mV (data overview in Table S.M. 2). To minimize the protocol duration, a scan rate value of 100 mV/s was finally selected. The slightly better performances of the electrodes modified with shorter protocols (5 cycles at 100 mV/S) might be explained by the polymerization solution. Indeed, the SDS solution has a very low surface tension and tend to spread on the electrode surface. Longer electropolymerization times might result in an uneven deposition since the monomer has more time to diffuse away from the WE surface.

The EIS data proved once again that the modified electrodes are still very conductive and indirectly report the successful modification of the electrode surface. The Nyquist plot for the modified electrodes can be fitted by the electrochemical equivalent circuit (EEC) reported in Fig. 2E. Two blocks of circuit elements can be identified; Rs is the uncompensated solution resistance while the first block [CPE 1, Rct 1] models the poly(Py-2-COOH) film and the second [CPE 2 (Rct 2 W)] is related to the electrode surface underneath the polymer. This circuit has been previously reported as a model for electrodes modified with materials with different conductivities and morphology of the underlying working electrode [47–49]. Thus, the final modification protocol encompass the electropolymerization of 10 mM of Py-2-COOH in 0.1 M SDS for 5 CV cycles at 100 mV/s. The resulting polymeric film provides the carboxylic acid functional groups needed for the covalent immobilization of biomolecules and improves the conductivity of the working electrode, as evidenced also by the EIS characterization.
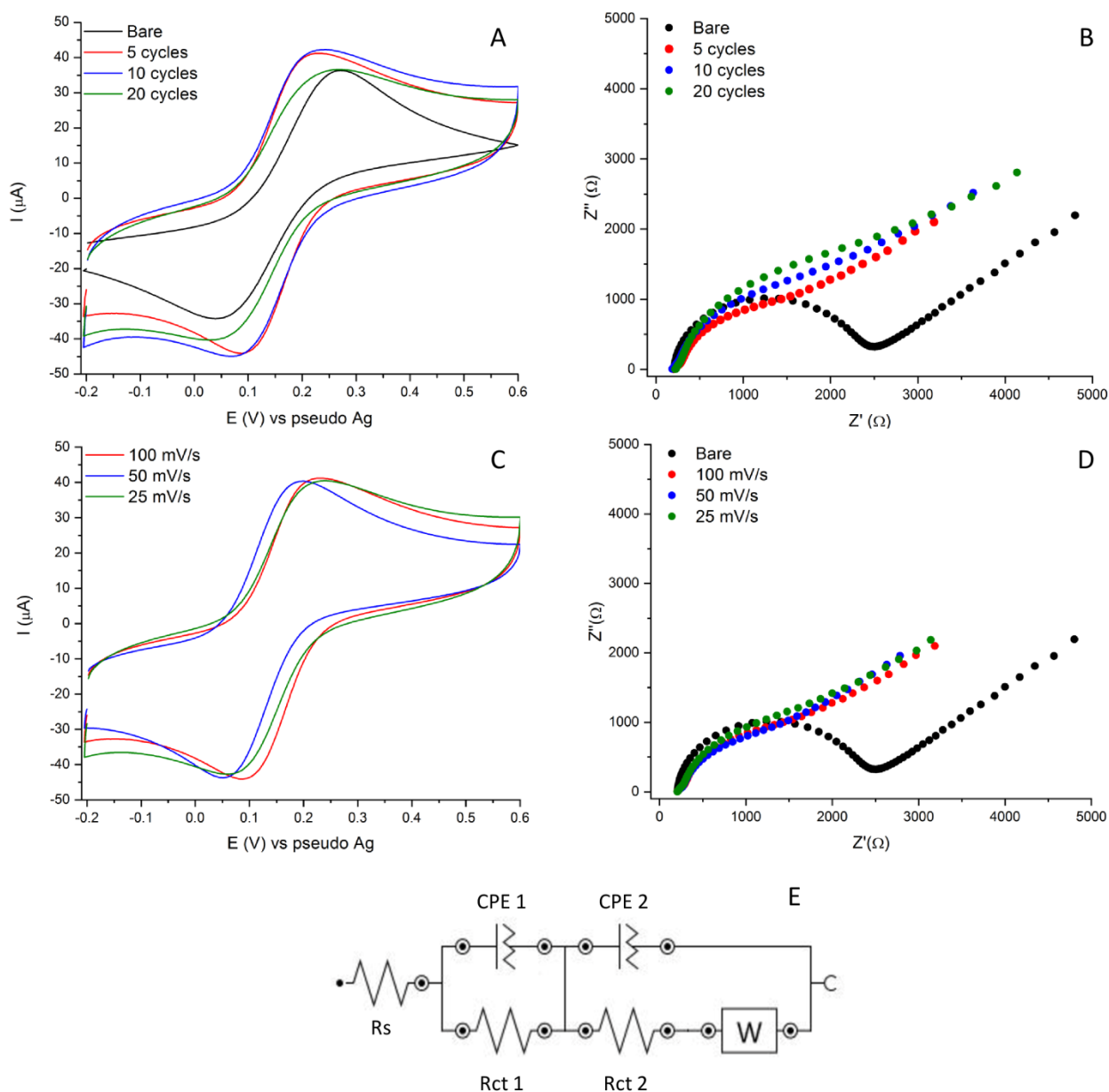
Fig. 2 Comparison of different electropolymerization parameters for 10 mM Py-2-COOH in 0.1 M SDS: CVs (A) and Nyquist plots (B) of G-SPEs after 5, 10 and 20 CV electropolymerization cycles at 100 mV/s; CVs (C) and Nyquist plots (D) of G-SPEs after 5 CV cycle electropolymerization at 25, 50 and 100 mV/s; (E) Schematic representation of the EEC used to fit the data. All the measurement were performed in 0.1 M KNO_3 with 2 mM $[Fe(CN)_6]^{3-/4-}$.

3.2 Impedimetric characterization of hSA-PFOA binding

The possibility to follow the formation of the hSA-PFOA complex was investigated by EIS at the surface of the modified G-SPE. The electrode surface rich in carboxylic acid functionalities was activated by EDC/NHS for the covalent immobilization of delipidated hSA. The chosen immobilization protocol was developed specifically for application at G-SPE, as previously reported by Rengaraj *et al.* [39]. Preliminary test showed that the optimal hSA loading was achieved with a 2 mg/mL solution (as reported in Fig. S.M. 4). Then, different concentration of PFOA were let in contact with the hSA-modified electrodes prior to characterizing the changes in the surface properties by EIS.

3.2.1 Characterization of the hSA-Py-2-COOH modified G-SPE

The Nyquist plots obtained at the bare G-SPE (bare, black dots) and after Py-2-COOH electropolymerization (Py-2-COOH, red dots), delipidated hSA immobilization (hSA, blue dots) and PFOA incubation (PFOA 1 µM, green dots) are reported in Fig. 3. To extract qualitative and quantitative information about the processes occurring at the electrode surface, the Nyquist plots were fitted with EEC reported in Fig. 3B and C.
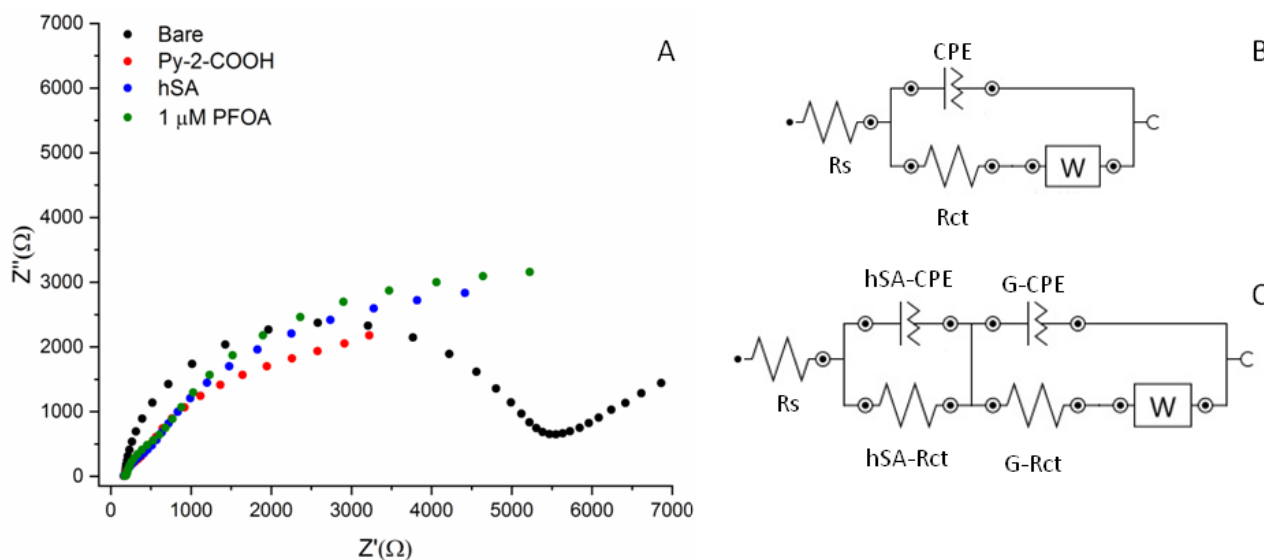
Fig. 3 A) Nyquist plots for bare (black dots), poly(Py-2-COOH) modified G-SPE (red dots) and hSA poly(Py-2-COOH) modified G-SPE in absence (blue dots) and presence of 1 µM PFOA (green dots), B) modified Randles EEC; C) hSA modified electrode EEC. All the measurement were performed in 0.1 M KNO_3 with 2 mM $[Fe(CN_6)]^{3-/4-}$.

The Nyquist plot for the bare G-SPE was fitted with the modified Randles circuit, reported in Fig 3B. In this circuit, the migration of charge through the electrolyte solution is described by the solution resistance (Rs), the double-layer formation at the electrode surface is modelled by a constant phase element (CPE), the charge-transfer reaction at the electrode corresponds to the Rct, and the linear diffusion from the bulk of the solution is modelled by the Warburg impedance element (W). The bare G-SPE presented a relatively high Rct (2.12 kΩ). After the electropolymerization of the conductive pyrrole-2-carboxylic acid film, the Rct was halved (1.02 kΩ). Moreover, the polymeric layer resulted to be highly reproducible and even G-SPEs with different initial Rct values showed comparable performance after the electropolymerization. The immobilization of the delipidated hSA led to the formation of a conductive layer. To model this modification, a different EEC, reported in Fig. 3C, with an additional resistor and capacitor in parallel was used. A similar EEC was previously reported by Xie *et al.* in the EIS study of bovine serum albumin absorption at platinum electrodes [50]. The additional elements (hSA-CPE and hSA-Rct) model the resistance and capacitance of the conductive delipidated hSA film. Indeed, the charge must pass through the protein film before accessing the electrode surface (the part consisting of G-CPE, G-Rct and W). The Nyquist plot obtained after the incubation of 1 µM PFOA (green dots) presents an increase in the semicircle part of the plot at lower frequencies which is linked to an increase in Rct of the layer. Thus, it is possible to hypothesize a direct influence of the PFOA on the hSA structure on the electrode surface. The conformational changes of delipidated hSA in presence of PFOA were further investigated by SEC-SAXS. The results (reported in S.M. par. 2) suggest that PFOA compacts the structure of albumin leading to a meaningful decrease of the radius of gyration (Rg). However, it is worth to notice that no denaturation or

protein unfolding was observed for hSA after incubation with PFOA. These data can be explained by considering the fatty-acid mimic behaviour of this contaminant that in presence of a completely delipidated protein is able to create strong interactions in the cavities that normally host lipids, hormones or drugs [51,52]. The structure assumed by the hSA in presence of PFOA might be responsible for the increase in Rct of the modified electrode; the redox mediator in solution will find its path towards the electrode surface hindered by the more compact hSA layer and thus resulting in an increased charge transfer resistance.

3.2.2 PFOA impedimetric analytical detection strategy

To simplify the detection strategy and improve the sensitivity of the sensors, a direct evaluation of the impedance signal changes was performed on the Bode phase plot instead of analysing the fitted parameters obtained from the EEC. From the Bode phase plot in Fig. 4A, recorded at the hSA-G-SPE (blue line), it was possible to identify two peaks, with Θ_{max} at 1 and 10 Hz, respectively. Each peak corresponds to a separate kinetic process with different time constants [53]. These processes were ascribed to the interaction of the redox mediator with the hSA and the polymeric film on the electrode surface. After incubation with PFOA containing solutions, the Θ_{max} of the process at 10 Hz increased (green line in Fig. 4A), suggesting that the presence of the contaminant changes the interaction between the hSA on the electrode surface and the redox mediator in solution. To use this event as analytical signal, the changes in the absolute impedance IZI [54], recorded at a fixed frequency of 10 Hz, were plotted against different PFOA concentrations, incubated at hSA-Py-2-COOH-G-SPE. The analytical parameter used is ΔZ, which is defined as the difference between the Z value of the hSA modified electrode at 10 Hz and the same value recorded after incubation with different PFOA solutions (ΔZ = $|Z|_{PFOA}$ - $|Z|_{hSA}$).
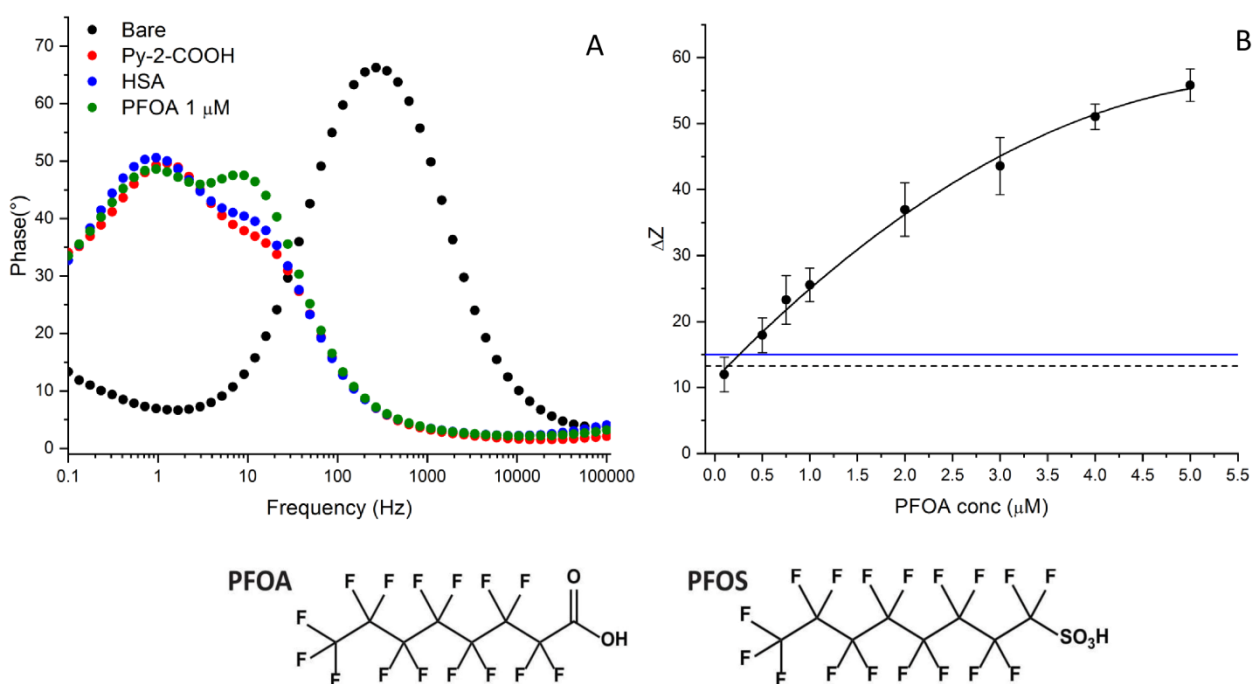
Figure 4. A) Bode phase plot for the hSA-Py-2-COOH-G-SPE recorded in 0.1 M phosphate buffer pH 7.4 with 2 mM $[Fe(CN_6)]^{3-/4-}$, bare (black dots), after Py-2-COOH electropolymerization (red dots), after hSA immobilization (blue dots) and after incubation with 1 μM PFOA (green dots); B) Calibration plot for the hSA-Py-2-COOH-G-SPE biosensors between 100 nM and 5 μM PFOA, average signal for 5 incubations of pure buffer (dashed black line), average signal for 5 incubation of 1 μM PFOS solution (blue full line), polynomial fitting equation: y = 11.20 + 14.97x^1 - 1.23x^2. Error bars calculated on triplicates. Inset: PFOA (left) and PFOS (right) molecular structures.

A calibration plot (Fig. 4B) was built in the range from 100 nM to 5 µM and the polynomial fitting of the data points had a R^2 of 0.997. PFOA concentrations higher than 2 µM result in the saturation of the bioreceptor. However, there is a possible linear interval between 500 nM and 2 µM. The error associated with the reproducibility of the impedimentric biosensors is c.a. 10%. As negative control tests, the hSA-G-SPE was incubated also with pure buffer (dashed black line in Fig. 4B) and 1 µM PFOS solution (full blue line in Fig. 4B). The average of 5 repeated measurements showed that the mean signals for both pure buffer and PFOS is lower then the value obtained with 500 nM of PFOA. The signal for 100 nM of PFOA falls below these threshold values and thus cannot be considered specific. These preliminary results showed the feasibility of an impedimetric-based PFOA detection strategy owing to its interactions with delipidated hSA.

5. Conclusion

Herein, the electropolymerization of a conductive poly(Py-2-COOH) modifier was optimized at G-SPE in 0.1 M SDS. The choice of this electrolyte assured reproducible and conductive polymer films on the screen-printed surface. Delipidated hSA was then covalently immobilized at the modified electrode via EDC/NHS coupling and the resulting modification was characterized by EIS. The obtained biosensing platform was tested in presence of increasing concentrations of PFOA and the changes at interfacial electron transfer were correlated to the formation of the hSA-PFOA complex. Extracting the absolute impedance values at 10 Hz from the Bode phase plot was possible to build a calibration plot in the nanomolar range. A possible interpretation of these impedimetric results was supported the study of the hSA-PFOA complex performed by SEC-SAXS analysis. This proof-of-concept study showed the ease of combining proteins bioreceptors with Py-2-COOH-G-SPE for PFOA monitoring in water samples. The applicability of this sensing strategy can be further improved by adding other surface electrode modifiers, such as nanomaterials or electroactive labels, to enhance the sensitivity or modifying the hSA receptor with protein engineering techniques.

6. Acknowledgments

References

[1]   G. Moro, K. De Wael, L.M. Moretto, Challenges in the electrochemical (bio)sensing of nonelectroactive food and environmental contaminants, Curr. Opin. Electrochem. 16 (2019) 57–65.

[2]   X. Dauchy, Per- and polyfluoroalkyl substances (PFASs) in drinking water: Current state of the science, Curr. Opin. Environ. Sci. Heal. 7 (2019) 8–12.

[3]   Y. Pan, J. Wang, L.W.Y. Yeung, S. Wei, J. Dai, Analysis of emerging per- and polyfluoroalkyl substances: Progress and current issues, TrAC Trends Anal. Chem. (2019) 115481.

[4]   S. Liu, R. Yang, N. Yin, Y.-L. Wang, F. Faiola, Environmental and human relevant PFOS and PFOA doses alter human mesenchymal stem cell self-renewal, adipogenesis and osteogenesis, Ecotoxicol. Environ. Saf. 169 (2019) 564–572.

[5]   M. Zhang, P. Wang, Y. Lu, X. Lu, A. Zhang, Z. Liu, Y. Zhang, K. Khan, S. Sarvajayakesavalu, Bioaccumulation and human exposure of perfluoroalkyl acids (PFAAs) in vegetables from the largest vegetable production base of China, Environ. Int. 135 (2020) 105347.

[6]   A. Cordner, V.Y. De La Rosa, L.A. Schaider, R.A. Rudel, L. Richter, P. Brown, Guideline levels for PFOA and PFOS in drinking water: the role of scientific uncertainty, risk assessment decisions, and social factors, J. Expo. Sci. Environ. Epidemiol. 29 (2019) 157–171.

[7]   D. Banks, B.-M. Jun, J. Heo, N. Her, C.M. Park, Y. Yoon, Selected advanced water treatment technologies for perfluoroalkyl and polyfluoroalkyl substances: A review, Sep. Purif. Technol. 231 (2020) 115929.

[8]   P.C. Ferreira, V.N. Ataíde, C.L. Silva Chagas, L. Angnes, W.K. Tomazelli Coltro, T.R. Longo Cesar Paixão, W. Reis de Araujo, Wearable electrochemical sensors for forensic and clinical applications, TrAC Trends Anal. Chem.

119 (2019) 115622.

[9]   L. Lu, Z. Zhu, X. Hu, Multivariate nanocomposites for electrochemical sensing in the application of food, TrAC Trends Anal. Chem. 118 (2019) 759–769.

[10]   C. Fang, Z. Chen, M. Megharaj, R. Naidu, Potentiometric detection of AFFFs based on MIP, Environ. Technol. Innov. 5 (2016) 52–59.

[11]   S. Chen, A. Li, L. Zhang, J. Gong, Molecularly imprinted ultrathin graphitic carbon nitride nanosheets–based electrochemiluminescence sensing probe for sensitive detection of perfluorooctanoic acid, Anal. Chim. Acta. 896 (2015) 68–77.

[12]   J. Gong, T. Fang, D. Peng, A. Li, L. Zhang, A highly sensitive photoelectrochemical detection of perfluorooctanic acid with molecularly imprinted polymer-functionalized nanoarchitectured hybrid of AgI–BiOI composite, Biosens. Bioelectron. 73 (2015) 256–263.

[13]   F. Cao, L. Wang, Y. Tian, F. Wu, C. Deng, Q. Guo, H. Sun, S. Lu, Synthesis and evaluation of molecularly imprinted polymers with binary functional monomers for the selective removal of perfluorooctanesulfonic acid and perfluorooctanoic acid, J. Chromatogr. A. 1516 (2017) 42–53.

[14]   L. Zheng, Y. Zheng, Y. Liu, S. Long, L. Du, J. Liang, C. Huang, M.T. Swihart, K. Tan, Core-shell quantum dots coated with molecularly imprinted polymer for selective photoluminescence sensing of perfluorooctanoic acid, Talanta. 194 (2019) 1–6.

[15]   N. Cennamo, L. Zeni, P. Tortora, M.E. Regonesi, A. Giusti, M. Staiano, S. D'Auria, A. Varriale, A high sensitivity biosensor to detect the presence of perfluorinated compounds in environment, Talanta. 178 (2018) 955–961.

[16]   X. Liu, M. Fang, F. Xu, D. Chen, Characterization of the binding of per- and poly-fluorinated substances to proteins: A methodological review, TrAC Trends Anal. Chem. 116 (2019) 177–185.

[17]   M. Salvalaglio, I. Muscionico, C. Cavallotti, Determination of energies and sites of binding of PFOA and PFOS to human serum albumin, J. Phys. Chem. B. 114 (2010) 14860–14874.

[18]   Q. Chi, Z. Li, J. Huang, J. Ma, X. Wang, Interactions of perfluorooctanoic acid and perfluorooctanesulfonic acid with serum albumins by native mass spectrometry, fluorescence and molecular docking, Chemosphere. 198 (2018) 442–449.

[19]   C. He, M. Xie, F. Hong, X. Chai, H. Mi, X. Zhou, L. Fan, Q. Zhang, T. Ngai, J. Liu, A highly sensitive glucose biosensor based on gold nanoparticles/bovine serum albumin/Fe3O4 biocomposite nanoparticles, Electrochim. Acta. 222 (2016) 1709–1715.

[20]   Z. Tang, Y. Fu, Z. Ma, Bovine serum albumin as an effective sensitivity enhancer for peptide-based amperometric biosensor for ultrasensitive detection of prostate specific antigen, Biosens. Bioelectron. 94 (2017) 394–399.

[21]   J.S. Daniels, N. Pourmand, Label-free impedance biosensors: opportunities and challenges, Electroanalysis. 19 (2007) 1239–1257.

[22]   F. Ghorbani Zamani, H. Moulahoum, M. Ak, D. Odaci Demirkol, S. Timur, Current trends in the development of conducting polymers-based biosensors, TrAC Trends Anal. Chem. 118 (2019) 264–276.

[23]   M.H. Naveen, N.G. Gurudatt, Y.B. Shim, Applications of conducting polymer composites to electrochemical sensors: A review, Appl. Mater. Today. 9 (2017) 419–433.

[24]   A.C. Gálvez-Iriqui, M.O. Cortez-Rocha, A. Burgos-Hernández, M. Calderón-Santoyo, W.M. Argüelles-Monal, M. Plascencia-Jatomea, Synthesis of chitosan biocomposites loaded with pyrrole-2-carboxylic acid and assessment of their antifungal activity against Aspergillus niger, Appl. Microbiol. Biotechnol. 103 (2019) 2985–3000.

[25]   J. Qin, D.G. Jo, M. Cho, Y. Lee, Monitoring of early diagnosis of Alzheimer's disease using the cellular prion protein and poly(pyrrole-2-carboxylic acid) modified electrode, Biosens. Bioelectron. 113 (2018) 82–87.

[26]   A. Kausaite-Minkstimiene, L. Glumbokaite, A. Ramanaviciene, E. Dauksaite, A. Ramanavicius, An amperometric glucose biosensor based on poly (pyrrole-2-carboxylic acid)/glucose oxidase biocomposite, Electroanalysis. 30 (2018) 1634–1644.

[27]   M. Foschini, H.S. Silva, R.A. Silva, A. Marletta, D. Gonçalves, Theoretical and experimental studies on the electronic, optical, and structural properties of poly-pyrrole-2-carboxylic acid films, Chem. Phys. 425 (2013) 91–95.

[28]   G. Sabouraud, S. Sadki, N. Brodie, The mechanisms of pyrrole electropolymerization, Chem. Soc. Rev. 29 (2002) 283–293.

[29]   G.K. Chandler, D. Pletcher, The electrodeposition of metals onto polypyrrole films from aqueous solution, J. Appl. Electrochem. 16 (1986) 62–68.

[30]   T.F. Otero, J. Rodríguez, Parallel kinetic studies of the electrogeneration of conducting polymers: mixed materials, composition and properties control, Electrochim. Acta. 39 (1994) 245–253.

[31]   L.F. Warren, D.P. Anderson, Polypyrrole films from aqueous electrolytes: the effect of anions upon order, J. Electrochem. Soc. 134 (1987) 101–105.

[32] Y. Li, J. Yang, Effect of electrolyte concentration on the properties of the electropolymerized polypyrrole films, J. Appl. Polym. Sci. 65 (2002) 2739–2744.

[33] J.M. Pernaut, R.C.D. Peres, V.F. Juliano, M.-A. De Paoli, Electrochemical study of polypyrrole/dodecyl sulphate, J. Electroanal. Chem. Interfacial Electrochem. 274 (1989) 225–233.

[34] D.-H. Han, H.J. Lee, S.-M. Park, Electrochemistry of conductive polymers XXXV: Electrical and morphological characteristics of polypyrrole films prepared in aqueous media studied by current sensing atomic force microscopy, Electrochim. Acta. 50 (2005) 3085–3092.

[35] H. Chen, P. He, H. Rao, F. Wang, H. Liu, J. Yao, Systematic investigation of the toxic mechanism of PFOA and PFOS on bovine serum albumin by spectroscopic and molecular modeling, Chemosphere. 129 (2015) 217–224.

[36] R.F. Chen, Removal of fatty acids from serum albumin by charcoal treatment., J. Biol. Chem. 242 (1967) 173–181.

[37] B.A. Boukamp, Practical application of the Kramers-Kronig transformation on impedance measurements in solid state electrochemistry, Solid State Ionics. 62 (1993) 131–141.

[38] P. Agarwal, M.E. Orazem, L.H. Garcia-Rubio, Application of measurement models to impedance spectroscopy III . Evaluation of consistency with the Kramers-Kronig relations, J. Electrochem. Soc. 142 (1995) 4159–4168.

[39] S. Rengaraj, Á. Cruz-Izquierdo, J.L. Scott, M. Di Lorenzo, Impedimetric paper-based biosensor for the detection of bacterial contamination in water, Sensors Actuators B Chem. 265 (2018) 50–58.

[40] C.E. Blanchet, A. Spilotros, F. Schwemmer, M.A. Graewert, A. Kikhney, C.M. Jeffries, D. Franke, D. Mark, R. Zengerle, F. Cipriani, S. Fiedler, M. Roessle, D.I. Svergun, Versatile sample environments and automation for biological solution X-ray scattering experiments at the P12 beamline (PETRA III, DESY), J. Appl. Crystallogr. 48 (2015) 431–443.

[41] A. Panjkovich, D.I. Svergun, CHROMIXS: Automatic and interactive analysis of chromatography-coupled small-angle X-ray scattering data, Bioinformatics. 34 (2018) 1944–1946.

[42] D. Franke, M. V. Petoukhov, P. V. Konarev, A. Panjkovich, A. Tuukkanen, H.D.T. Mertens, A.G. Kikhney, N.R. Hajizadeh, J.M. Franklin, C.M. Jeffries, D.I. Svergun, ATSAS 2.8: A comprehensive data analysis suite for small-angle scattering from macromolecular solutions, J. Appl. Crystallogr. 50 (2017) 1212–1225.

[43] P. V. Konarev, V. V. Volkov, A. V. Sokolova, M.H.J. Koch, D.I. Svergun, PRIMUS: A Windows PC-based system for small-angle scattering data analysis, J. Appl. Crystallogr. 36 (2003) 1277–1282.

[44] Y. Wang, H. Yu, X. Shi, Z. Luo, D. Lin, M. Huang, Structural mechanism of ring-opening reaction of glucose by human serum albumin, J. Biol. Chem. 288 (2013) 15980–15987.

[45] D. Svergun, C. Barberato, M.H. Koch, CRYSOL - A program to evaluate X-ray solution scattering of biological macromolecules from atomic coordinates, J. Appl. Crystallogr. 28 (1995) 768–773.

[46] G. Moro, D. Cristofori, F. Bottari, E. Cattaruzza, K. De Wael, M.L. Moretto, Redesigning an Electrochemical MIP Sensor for PFOS: Practicalities and Pitfalls, Sensors. 19 (2019) 4433.

[47] A. Ramanavicius, A. Finkelsteinas, H. Cesiulis, A. Ramanaviciene, Electrochemical impedance spectroscopy of polypyrrole based electrochemical immunosensor, Bioelectrochemistry. 79 (2010) 11–16.

[48] C. Deslouis, M.M. Musiani, B. Tribollet, Free-standing membranes for the study of electrochemical reactions occurring at conducting polymer/electrolyte interfaces, J. Phys. Chem. 100 (1996) 8994–8999.

[49] M.A. Vorotyntsev, B. Tribollet, Comparison of the AC impedance of conducting polymer films studied as electrode-supported and freestanding membranes, J. Electrochem. Soc. 142 (1995) 1902–1908.

[50] Q. Xie, C. Xiang, Y. Yuan, Y. Zhang, L. Nie, S. Yao, A novel dual-impedance-analysis EQCM system—investigation of bovine serum albumin adsorption on gold and platinum electrode surfaces, J. Colloid Interface Sci. 262 (2003) 107–115.

[51] J. Ghuman, P.A. Zunszain, I. Petitpas, A.A. Bhattacharya, M. Otagiri, S. Curry, Structural basis of the drug-binding specificity of human serum albumin, J. Mol. Biol. 353 (2005) 38–52.

[52] A.A. Bhattacharya, T. Grüne, S. Curry, Crystallographic analysis reveals common modes of binding of medium and long-chain fatty acids to human serum albumin, J. Mol. Biol. 303 (2000) 721–732.

[53] E. Casero, A.M. Parra-Alfambra, M.D. Petit-Domínguez, F. Pariente, E. Lorenzo, C. Alonso, Differentiation between graphene oxide and reduced graphene by electrochemical impedance spectroscopy (EIS), Electrochem. Commun. 20 (2012) 63–66.

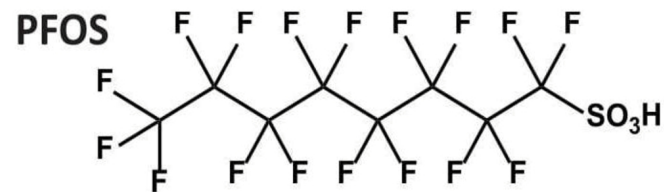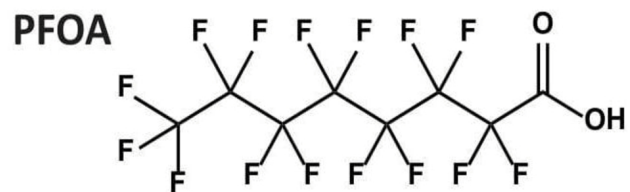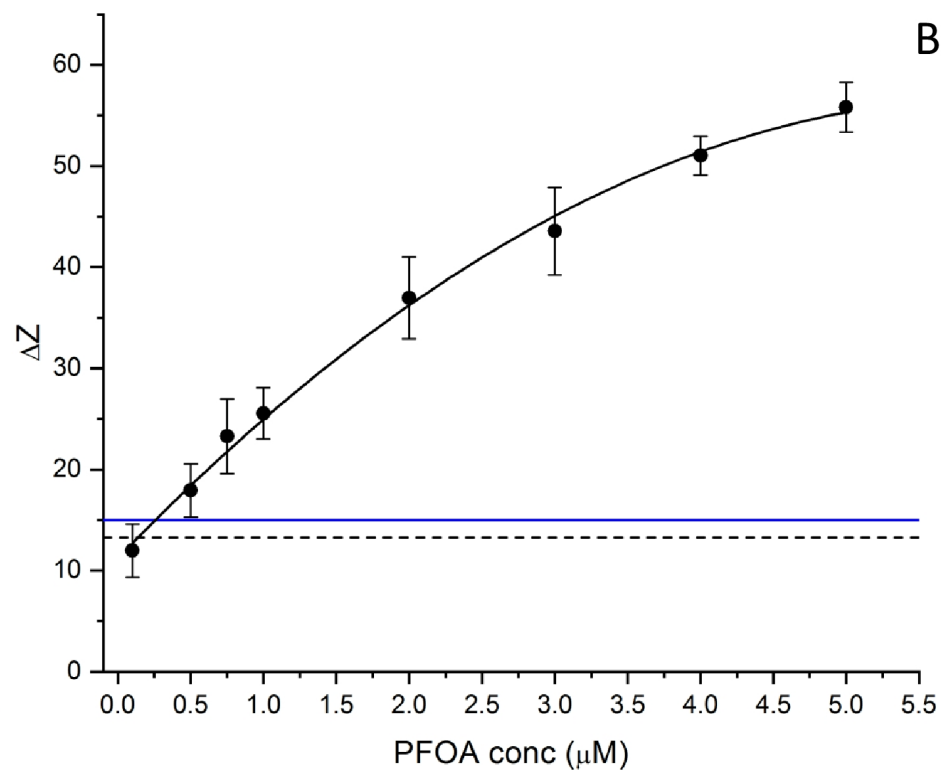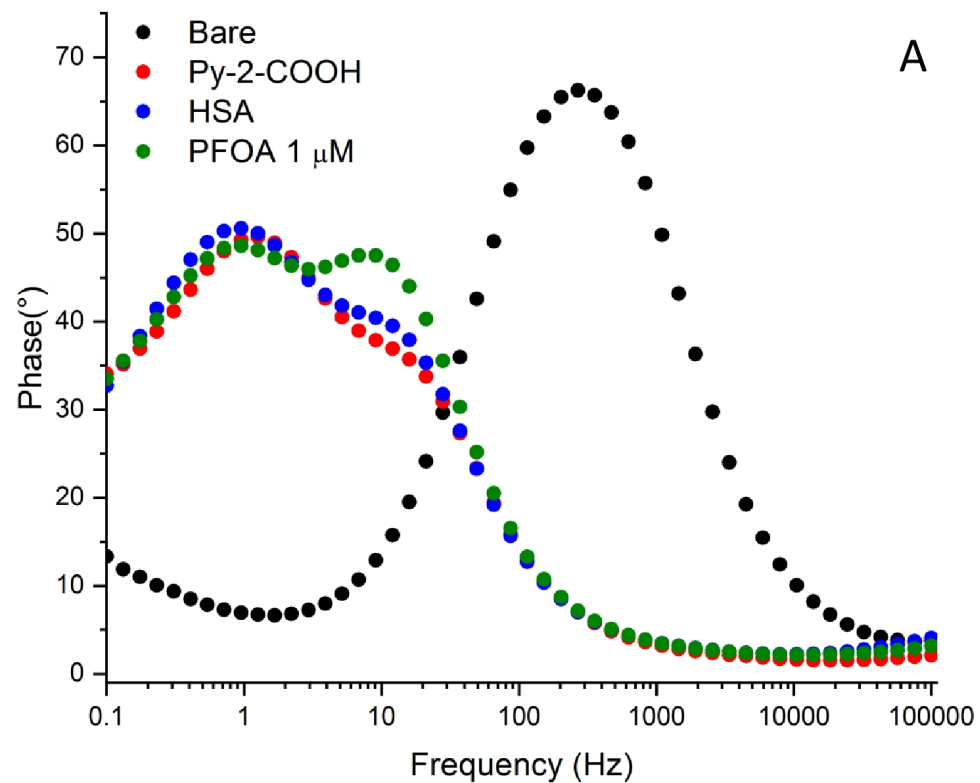[54] Vadim F. Lvovich, ed., Impedance Analysis of Complex Systems, in: Impedance Spectrosc., 2012: pp. 113–161.
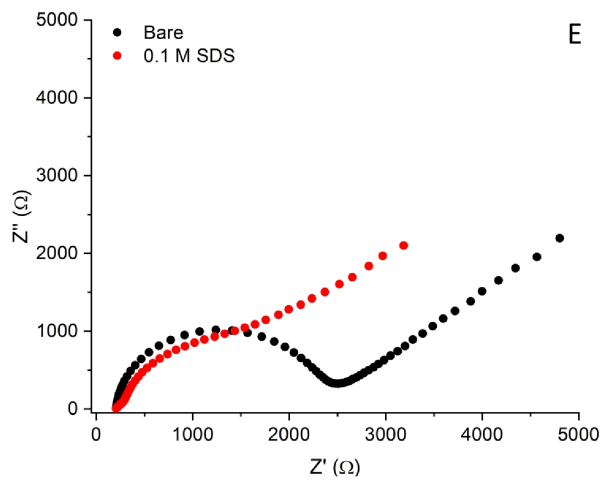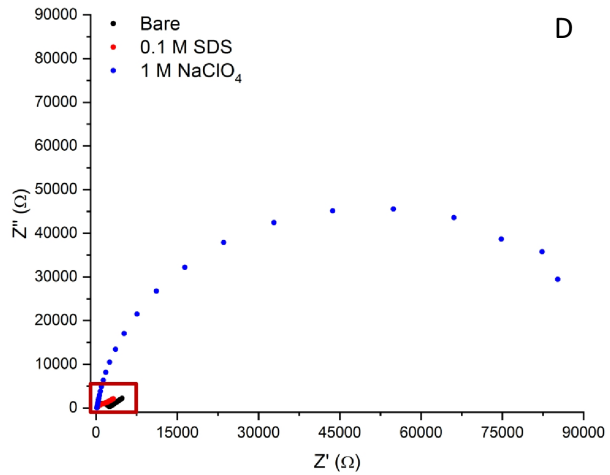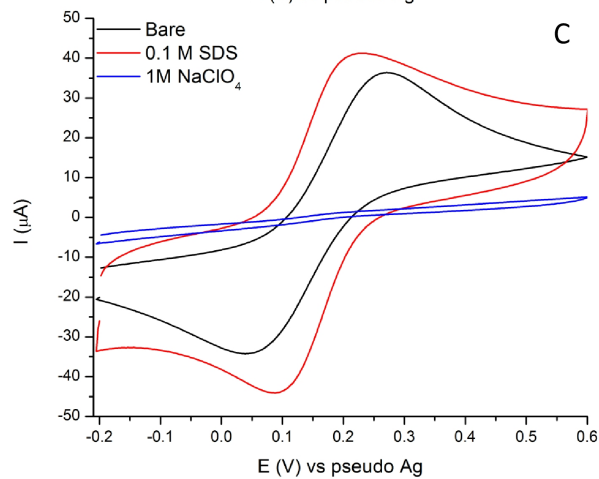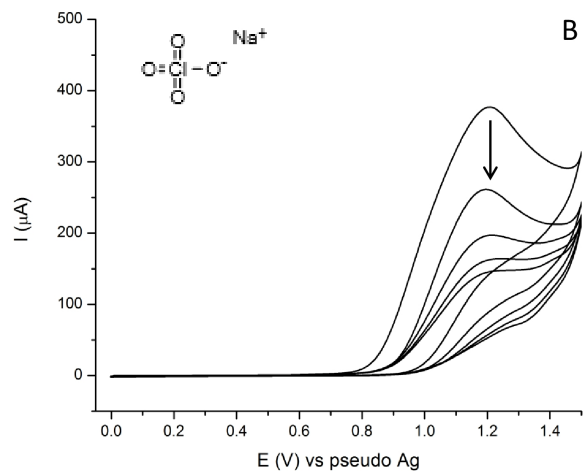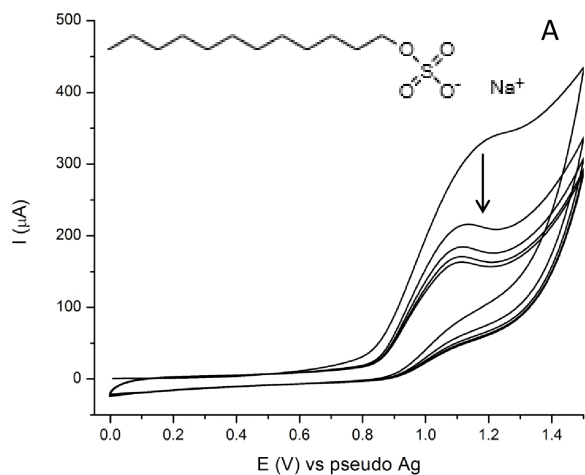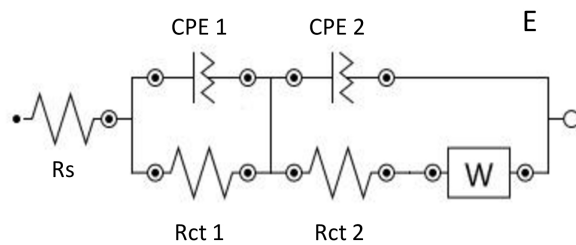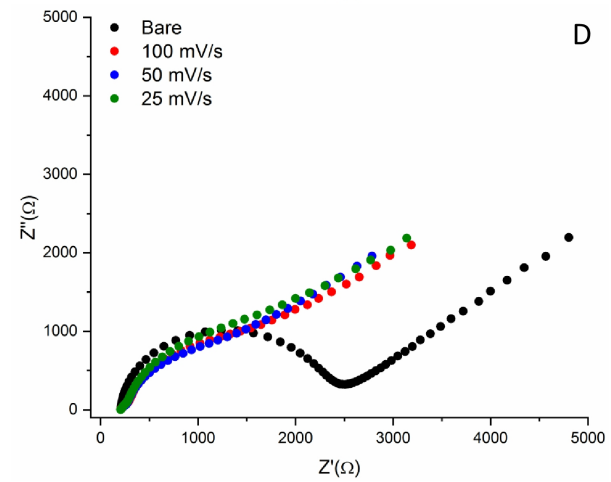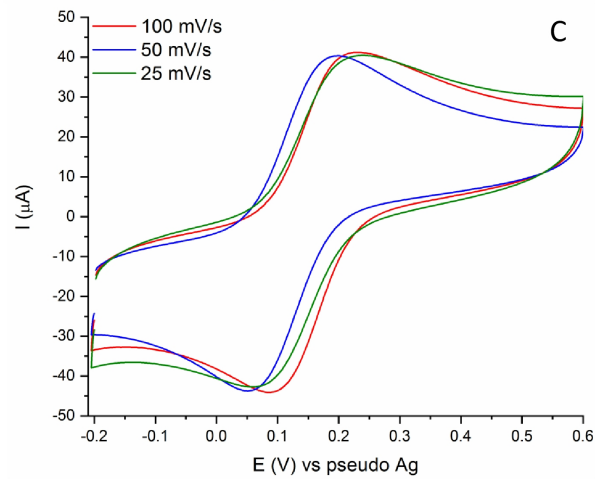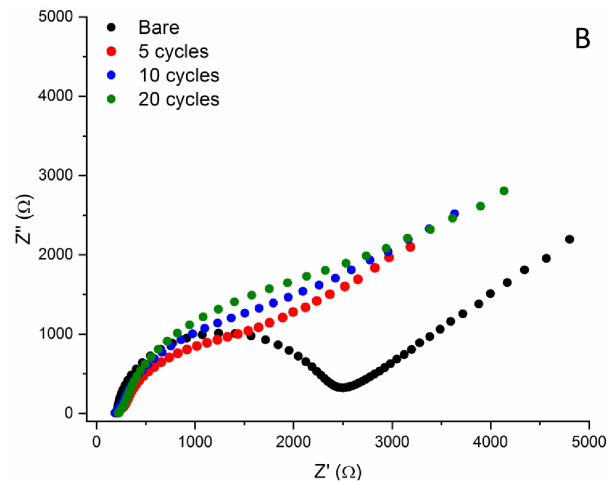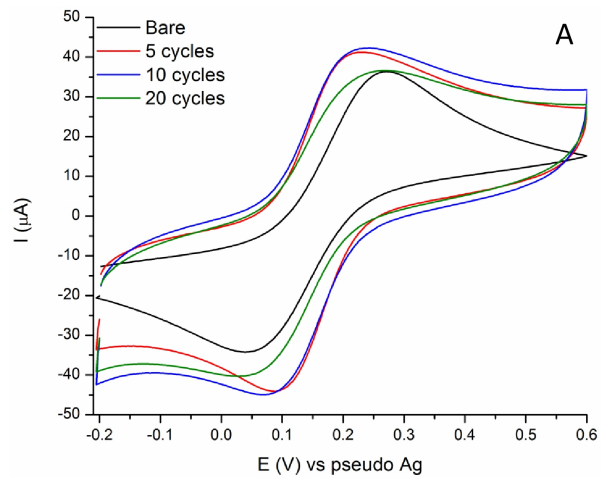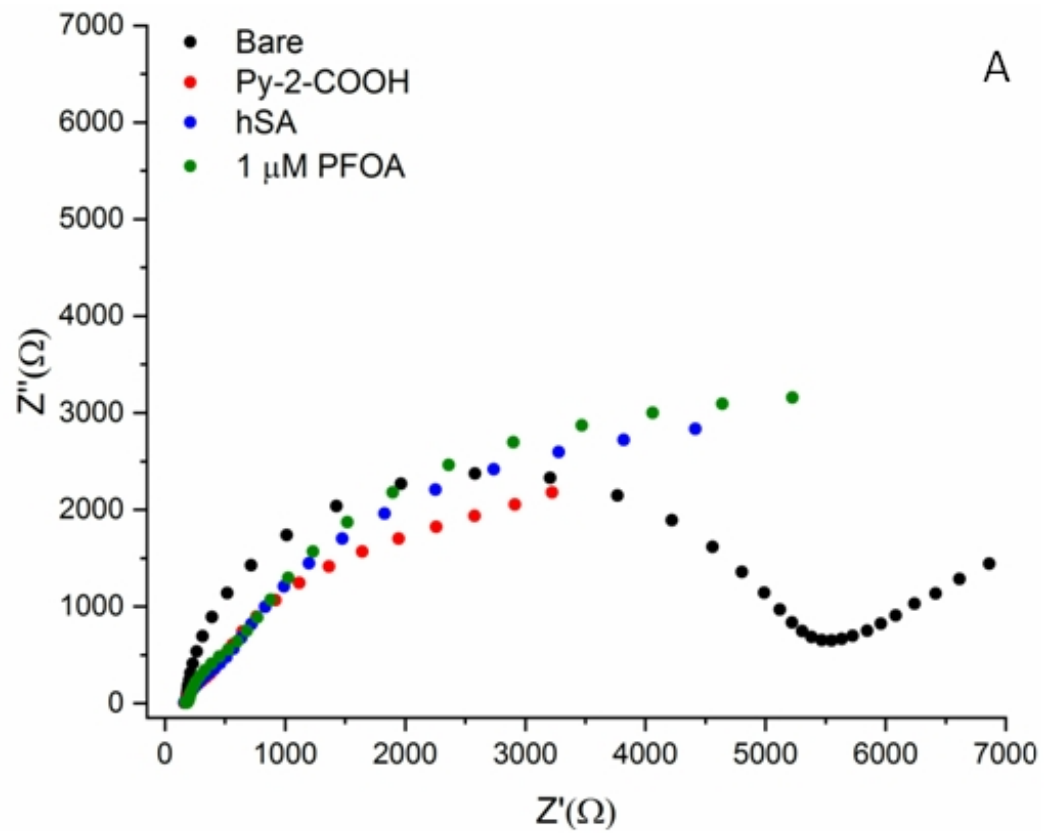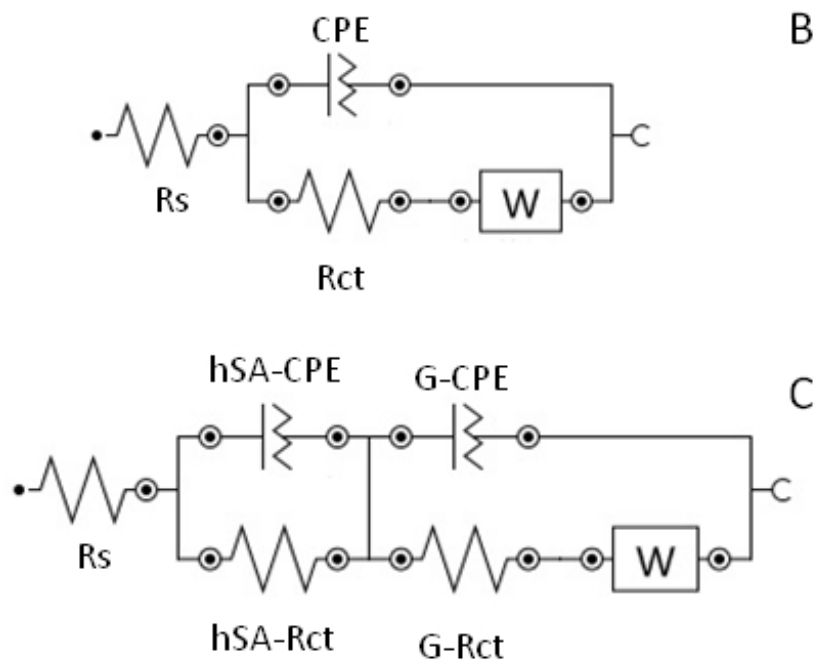
Conflict of interest statement

The authors declare no conflict of interests

Covalent immobilization of delipidated human serum albumin on poly(pyrrole-2-carboxylic) acid film for the impedimetric detection of perfluorooctanoic acid

Giulia Moro [a,b,c,1*], Fabio Bottari [b,c,1], Stefano Liberi [a], Sonia Covaceuszach [d], Alberto Cassetta [d], Alessandro Angelini [a,e], Karolien De Wael [b,c], Ligia Maria Moretto [a]

[a] Department of Molecular Sciences and Nanosystems, Ca' Foscari University of Venice, Via Torino 155, 30172 Mestre, Italy; [b] AXES Research Group, Department of Bioscience Engineering, University of Antwerp, Groenenborgerlaan 171, 2020 Antwerp, Belgium; [c] NANOlab Center of Excellence, Groenenborgerlaan 171, 2020 Antwerp, Belgium; [d] Istituto di Cristallografia – CNR, Trieste Outstation, Italy SS 14 km 163.5, Basovizza, Trieste, Italy; [e] European Centre for Living Technology (ECLT), Ca' Bottacin, Dorsoduro 3911, Calle Crosera, 30123 Venice, Italy.

[1] *These authors contributed equally to this work and should be considered co-first authors.*

Corresponding author: giulia.moro@unive.it

Table of contents:

1. *Morphological characterization of bare and modified graphite screen-printed electrodes by Scanning Electrode Microscopy (SEM)*

Figure S.M.1 reports the SEM images acquired at graphite screen-printed electrodes (G-SPE) before and after the pyrrole-2-carboxylic acid electropolymerization in SDS or $NaClO_4$ solution.

The surface of the bare G-SPE (A and B) presents a spongy texture, with irregular branched aggregates and a relatively high porosity.

Comparing the images acquired at the SDS modified G-SPE (C and D), it is possible to notice that the surface morphology remains unchanged. The polymer is possibly growing in a thin film (not necessarily continuous) that follows the rough pattern of the surface. As in the bare G-SPE, there are areas with slightly different conductivities (see lighter spots in B and D), suggesting that the polymers obtained in SDS solutions are not affecting the conductivity of G-SPE surface.

When $NaClO_4$ is used, SEM images (D and E) showed the formation of a more compact layer that results in a loss of surface porosity and can support the electrochemical characterization.
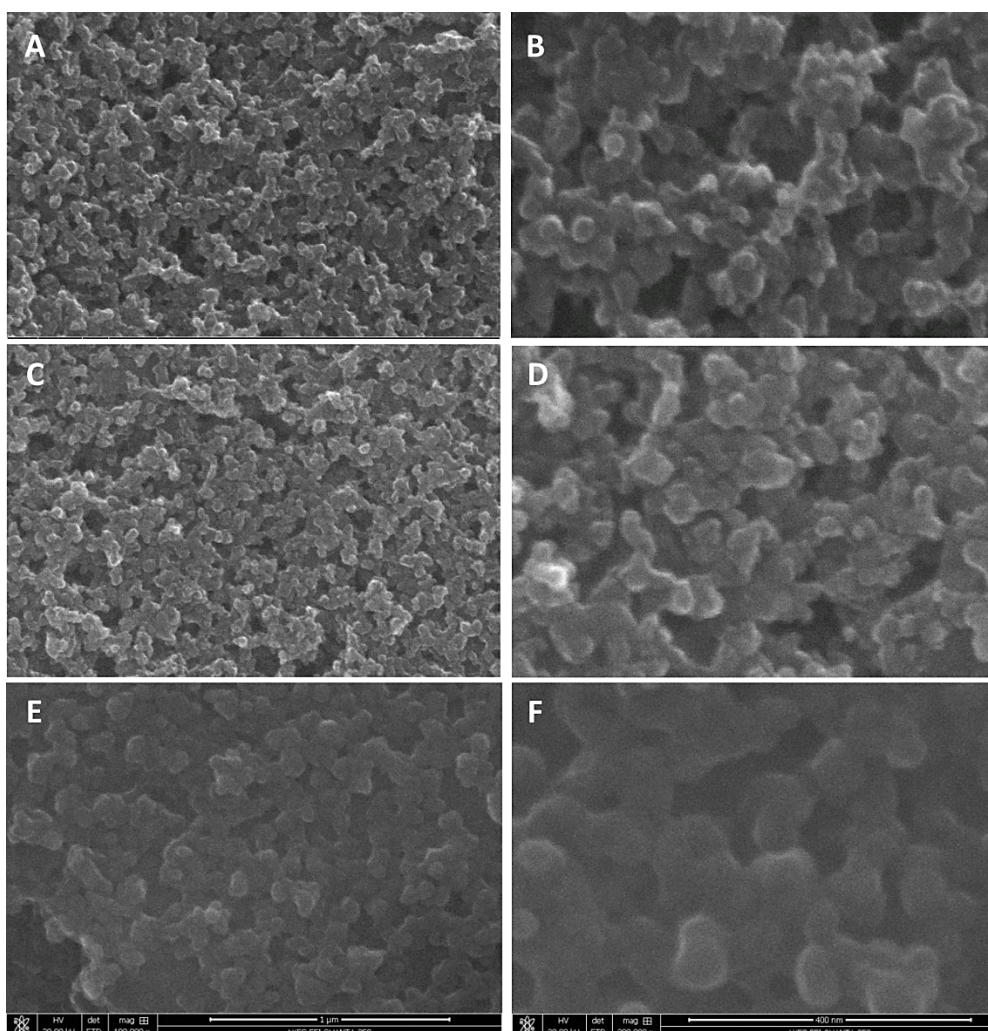

Fig. S.M. 1 SEM images acquired using secondary electrons at different magnification: 100 000x (left column) and 300 000x (right column) of the bare G-SPE (A and B) and after 5 cycles of electropolymerization with SDS (C and D) and $NaClO_4$ (E and F).

2. *PFOA binding influences on size parameters of delipidated hSA in solution as assessed by Size Exclusion Chromatography Small-angle X-ray scattering (SEC-SAXS) experiments.*

SEC-SAXS measurements were performed on delipidated hSA in unbound state, known as *apo form*, and in complex with 1 mM PFOA. The experimental SAXS curves are compared in Fig. S.M. 2A and the size parameters calculated from the raw data are summarized in Table S.M. 2. From these latter, it is possible to observe that the molecular masses (MM), calculated from the hydrated particle volumes (Vp), were consistent with values expected for monomeric species and in agreement with the MM estimated from the primary sequences, c.a. 66.5 kDa.

Even if the overall distance distribution function and therefore the calculated D_{max} are not affected by the interaction with PFOA, there is a meaningful change in the radius of gyration, Rg. This difference (about 0.8 Å) is clearly visible in the plots reported in Fig. S.M. 2B-C, suggesting a conformational change of delipidated hSA in presence of PFOA. In particular, PFOA-hSA complexes assumed a more compact shape in respect to the apo form, with a significant decrease in the Rg values (from 27.900 ± 0.006 Å for the apo protein to 27.100 ± 0.008 Å for the complex with PFOA).
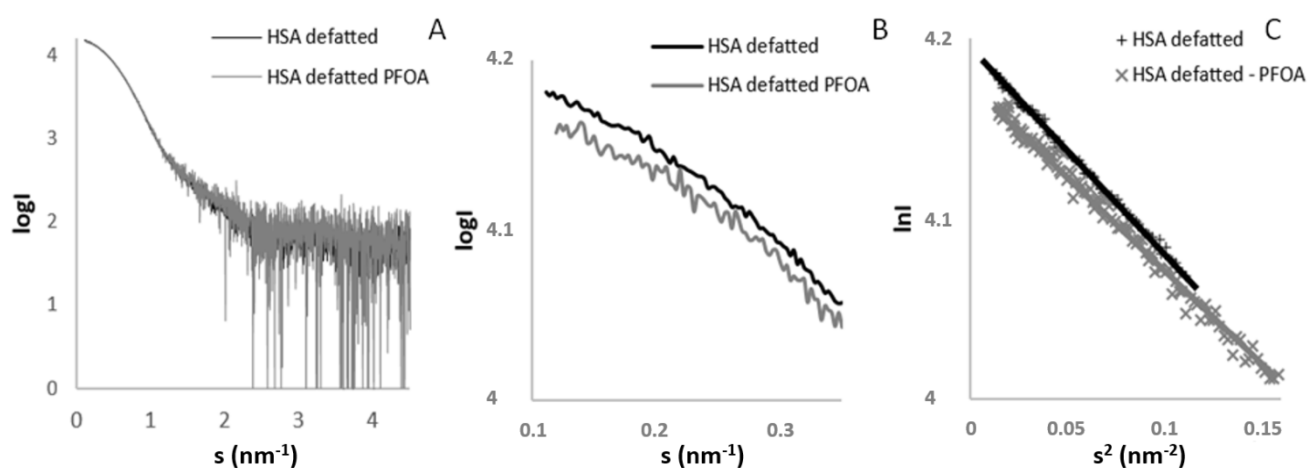

Fig. S.M. 2 A) Comparison of the experimental SEC-SAXS data obtained for the apo form of delipidated hSA and the complex with PFOA and B) the zoomed regions of these graphs at low angles; the plots display the logarithm of the scattering intensity (logI) as a function of momentum transfer (s); C) Comparison of Guinier plots and fits of the SEC-SAXS data for the apo form of delipidated hSA and the complex with PFOA.

Table S. M. 1 SAXS structural parameters: radius of gyration (*Rg*), maximum dimension (*Dmax*), Porod volume (*Vp*), and Molecular Mass (*MM*). *Dmax* was obtained from the distribution function using GNOM; I(0) (scattering intensity) was obtained from the scattering data by the Guinier analysis.

Data collection parameters	hSA delipidated	hSA delipidated/PFOA
Instrument	P12 (PETRA III)	
Beam geometry (mm^2)	0.2 x 0.12	
Wavelength (Å)	1.24	
s range (Å^{-1})	0.003–0.445	
Concentration (mg/ mL)	9	
Temperature (K)	283	
Structural parameters		
I(0) (A.U.) [from Guinier]	15584±10	7634±12
Rg (A) [from Guinier]	**27.900±0.006**	**27.100±0.008**
Guinier sRg limits	0.986	1.11
Dmax (Å)	80±4	
Vp Porod volume estimate (Å^3)	110390±10000	109550±10000
Molecular mass determination (Da)		
MM [from Porod volume]	64900±6000	64400±6000
Calculated monomeric MM from sequence	66500	

The observed conformational changes is confirmed by the comparison of the experimental scattering data with theoretical scattering curves (reported in Fig. S.M. 3) computed by CRYSOL [1] from the crystal structure of delipidated hSA [2]. A poor fit with a χ^2 of 3.79 was obtained for the apo form. This result is ascribed to the packing stabilizing interactions that take place in the crystal lattice, resulting in a crystallographic structure more compact than the respective conformation in solution.

On the contrary, PFOA binding induces a more compact conformation of delipidated hSA that is very close to the crystal structure with a good accordance (χ^2 of 1.54) between the calculated and measured scattering intensities.
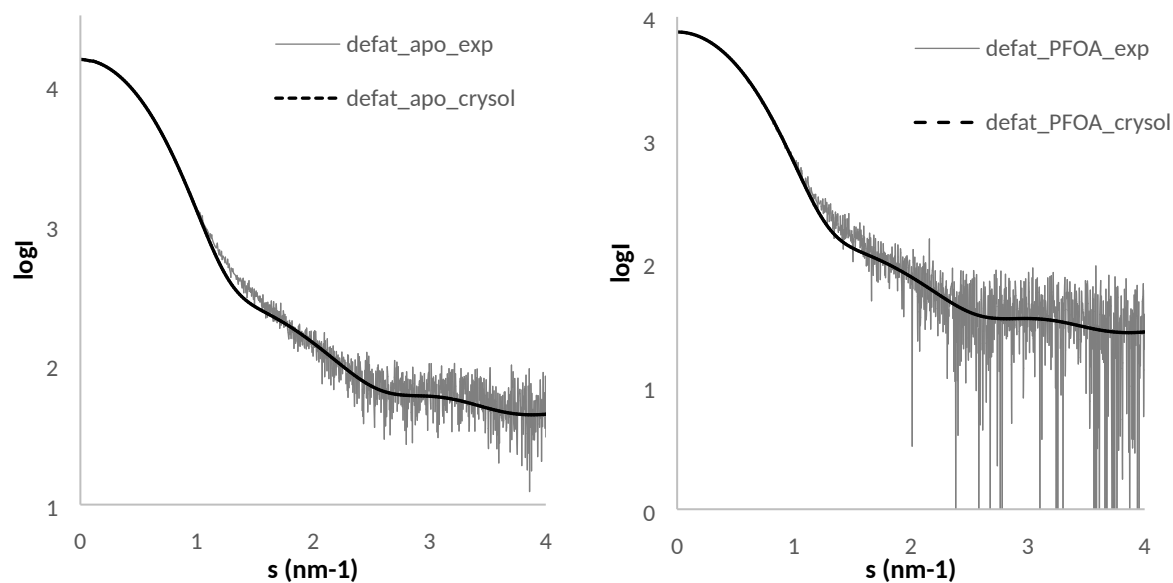
Fig. S.M. 3 Comparison of the crystallographic delipidated hSA (dashed line) with experimental SEC-SAXS data for the apo form (left) and for the complex with PFOA (right), data analysis performed with CRYSOL [1].

3. *Electrochemical data summary*

Table S. M. 2 Electrochemical parameters of the different poly(Py-2-COOH) modified electrodes: 5, 10 and 20 CV electropolymerization cycles recorded at 100 mV/s or 5 CV electropolymerization cycles recorded at 25, 50 and 100 mV/s. Average and STD were calculated from triplicate measurements.

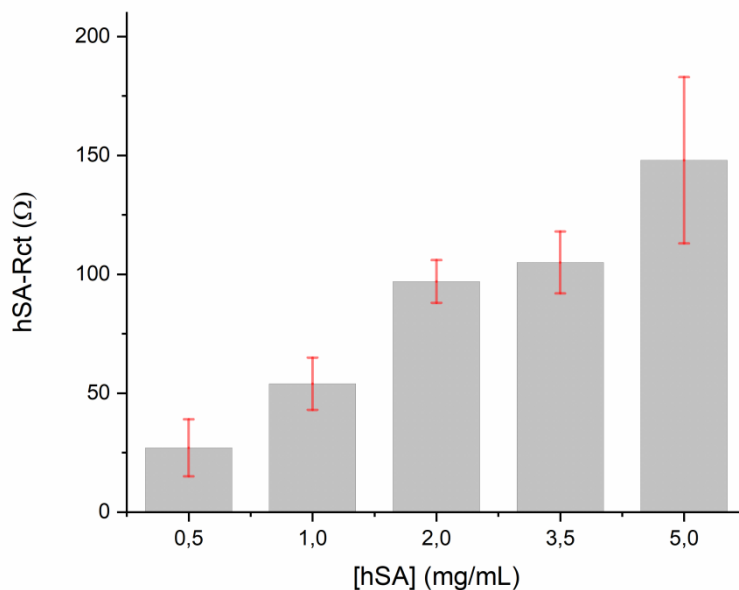|	ΔEp (mV)	Ipa/Ipc
Bare	202 ± 8	1.23
5 cycles	112 ± 4	1.03
10 cycle	122 ± 2	1.14
20 cycles	173 ± 5	1.16
25 mV/s	134 ± 6	1.11
50 mV/s	124 ± 3	1.10
100 mV/s	112 ± 4	1.03

4. *Optimization of hSA loading*

Fig. S.M. 4 Optimization of hSA loading on Py-2-COOH-G-SPE. Values of hSA-Rct at different protein concentrations (0.5, 1, 2, 3.5, 5 mg/ml). Average and STD were calculated from triplicate measurements. A limited range of hSA concentrations, from 0.5 to 5 mg/mL, was tested. The optimization was based on the comparison of the hSA-Rct values calculated by fitting the data with the EEC reported in Fig. 3C. We observed that with a hSA concentration lower than 2 mg/mL the associate Rct values were affected by a relatively high error suggesting a non-stable modification. With 2 mg/mL a good reproducibility was obtained, while for higher concentrations hSA-Rct did not change significantly. With 5 mg/mL we recorded an increase in the Rct but with a much higher associated error. Based on this consideration we consider 2 mg/mL the optimal concentration for hSA-loading at Py-2-COOH-G-SPE.

References

[1]   D. Svergun, C. Barberato, M.H. Koch, CRYSOL - A program to evaluate X-ray solution scattering of biological macromolecules from atomic coordinates, J. Appl. Crystallogr. 28 (1995) 768–773.

[2]   Y. Wang, H. Yu, X. Shi, Z. Luo, D. Lin, M. Huang, Structural mechanism of ring-opening reaction of glucose by human serum albumin, J. Biol. Chem. 288 (2013) 15980–15987.